MATERIALS DESTRUCTION THROUGH CAVITATION -

TESTS CARRIED OUT WITH HIGH FREQUENCY OSCILLATOR

by Dr. Hans Nowotny

Published by V.D.I. - Berlin, 1942

- - -

Translation from the German by Ferd Stenger, U.S.B.R.
Technical Library, Denver, March 1948

Introduction by W. Spannhake

For quite sometime I have felt the need for a thorough physico-chemical investigation of the phenomenon of cavitation. Although fundamental concepts were fairly well established by Föttinger, nonetheless, a large number of problems, especially those of material strength, required a solution. When Prof. Dr. L. Ebert, a former colleague at the Karlsruhe Technical High School, concurred with my proposal concerning this problem and placed at my disposal one of his coworkers, Dr. Nowotny, I was indeed grateful.

For providing the facilities our thanks go to Prof. Dr. Holler, Director of the Griesheim Works of the I. G. Farben Industries.

After a few conclusive tests carried out in a Venturi tube with a hydraulic flow strength of 400 horsepower, in which traces of cavitation could be detected within 30 seconds, we decided to make further tests using a high frequency oscillator. Only with this apparatus was it considered possible to study the cavitation problem under the influence of all measurable variables. For here a test specimen of less than 100 g may be subjected to oscillations of high frequencies in a cupful of any chosen liquid.

The results of the many tests carried out with various types of solids in different liquids are incorporated in this report. Not only do the results establish a classification, but the tests throw light upon the very beginning and upon the subsequent steps of materials erosion. Dr. Nowotny's tests have given a comprehensive concept of the progressive action of cavitation and the conclusions reached from the results (including the role of the chemical reactions) appear to me to be free from flaws. From the theoretical standpoint as well as in applied practice these results should prove of considerable significance.

I am sure that this book will be of great interest to those who have occasion to deal with the phenomenon of cavitation.

Karlsruhe, July 1941.

W. Spannhake, V.D.I.

TABLE OF CONTENTS

		Page No.
	Notations	iii
I.	Cavitation	
1.	Introduction	1
2.	Materials destruction through cavitation	2
3.	Testing method	4
4.	Resistance to cavitation and the mechanical properties of materials	6
5.	The periodicity in cavitation	9
II.	Gaines' Oscillator	
6.	Arrangement	9
7.	Cavitation produced by ultrasonic oscillator	11
8.	Methods of measurement and general observations	13
III.	Cavitation Attack	
9.	The vapor pocket formation at the boundary surface	14
10.	Damage brought about in water and aqueous solutions	16
11.	Damage brought about in organic liquids	18
12.	Degree of damage caused by oscillating vapor bubbles	20
13.	The relationship of the cavitation attack to pressure and temperature	21
14.	The dependency of the cavitation attack on the surface tension and the viscosity of the liquid	23

TABLE OF CONTENTS (Continued)

Page No.

15. The influence of the gas content 24

16. Formation of vapor bubbles and primary reaction 27

17. Chemical reactions in cavitation 31

IV. Resistance to Cavitation

18. The change brought about at the surface of the material by cavitation 33

19. The behavior of metallic materials 35

20. The behavior of nonmetallic materials 36

21. Structural change brought about by cavitation 36

22. Cavitation resistance--its dependence upon the properties of the material--a look into the future 39

V. Summary 42

List of References 44

NOTATIONS

The more important symbols and their physical units.

a (cm) = oscillating amplitude.

A ($g\ cm^2/sec^2$) = capillary work.

c (cm/sec) = velocity of sound.

d (cm) = diameter of bubble.

e ($g/cm\ sec^2$) = energy density (Energiedichte).

E ($g/cm\ sec^2$) = modulus of elasticity.

f (sec^{-1}) = frequency.

F = function.

g (cm/sec) = acceleration due to gravity.

k, k' = constants.

k_1 = cavitation number.

L (cm) = length of column, length of hollow space.

p ($g/cm\ sec^2$) = external pressure (total pressure).

p_a ($g/cm\ sec^2$) = pressure at the beginning of cavitation.

p_i ($g/cm\ sec^2$) = pressure within the bubble.

p_l ($g/cm\ sec^2$) = saturation pressure of the dissolved air in water.

p_s ($g/cm\ sec^2$) = saturation pressure (evidently vapor pressure - translator).

q_e ($g/cm\ sec^2$) = static pressure.

r (cm) = bubble radius.

r_o (cm) = bubble radius before collapse.

s (cm) = liner distance.

T (o_c) = absolute temperature.

v (cm/sec) = fluid velocity, velocity of the bubble.

v_{max} (cm/sec) = maximum fluid velocity.

v_t (cm/sec) = tangential fluid velocity.

ΔV (cm^3/sec) = volume loss per unit time.

α = air absorption in fluid (Bunsen's absorption coefficient).

α_s = air saturation in fluid.

η (g/cm sec) = viscosity.

ρ (g/cm^3) = density.

σ (g/sec^2) = surface tension.

I. CAVITATION

1. Introduction

The designers and the builders of hydraulic power machines have known for a long time of the destruction to machine parts when the pressure of the liquid p drops at the place in question to the vapor pressure p_s; i.e. $p = p_s$. In this case we have in place of a homogeneous liquid a dual phase condition, namely liquid and coexisting vapor. As a consequence there occurs cavitation, the pitting of the material. There are two phases to this phenomenon, the loss in energy and at the same time the destruction of the material. The causes for the attack on materials have as yet not been fully understood. In the beginning the problem was approached from the hydrodynamic side in which "outside" conditions were considered responsible for cavitation. By "outside" conditions are meant velocity and pressure with their dependency on time, especially with the development of oscillatory conditions. We, on the other hand, approached the problem with the "inner" conditions in mind which we considered necessary to show the mechanism of cavitation.

As early as 1887, Thomson (64) investigated the problem in connection with his experiments on stream flow. He foretold the loosening of materials at the walls and also predicted cavitation in a sphere by backflow. But a few years later deterioration in ship propellers and turbine buckets, etc., which were caused by cavitation, were considered as corrosion (8). The first attempt to approach this problem systematically was made by Föttinger (20).

In the study of the cavitation phenomena, the following experimental apparatus have developed in the course of time:

(1) The convergent-divergent tube (Föttinger) and the modified diffusor of Schröter (52).

(2) The water impact apparatus by Honegger (27) and that of de Haller (24).

(3) The ram arrangement of Ackeret and de Haller (5).

(4) The frequency oscillator of Gaines (22).

The simplest experimental apparatus is a smooth-walled convergent-divergent tube (venturi tube) with a glass observation window. This permits a precise follow-up of the flow condition during cavitation. In this arrangement one can note the rhythmic loosening of the stream from the divergent tube wall. Figure 1 shows the stream formation in a venturi tube in which the stream constriction and the formation of hollow spaces can be seen. There is also strong foam formation at the stream border and vapor formation in the hollow spaces. The collapse of the hollow spaces

according to E. Spannhake's investigations (61) occurs with a definite frequency f which bears a simple relationship to the stream velocity V_{max} in the narrowest cross section and the length of the hollow space L:

$$f = k\, V_{max}/L,$$

where k is the factor of proportionality. In order to convey the idea of the magnitude of the converted energy into sound, it may be remarked that in the case of the venturi chamber installed outdoors at the Schwarzenbachwerk with a water column of 350 m (1,150 feet) where V_{max} = 80 m/sec (260 ft/sec) the sound can be heard hundreds of meters away. The formation of the hollow spaces were also proven by means of oscillographic pressure measurements. Pressure measurements taken within the chamber in the initial stage of cavitation showed that pressures reach the magnitude of the vapor stresses in the divergent part of the chamber but drop immediately behind the narrowest cross section, however, materials destruction does not show in this region, but further on. (See Figure 2 and references 50 and 51.)

It was soon suspected that the "inner" conditions were connected with the presence of gas and vapor pockets which by exceedingly rapid densification could exert local impacts. The impression of the hollow space and vapor pockets formation led to the replacement of the term cavitation by the term Hohlsog (literally to suck hollow). In our discussion we shall drop this designation in favor of the older term, inasmuch as we shall show that, in general, the concept of cavitation covers not only the formation of hollow spaces but all other hydrodynamic phenomena connected with the unfavorable action upon materials. Frequently, the term water hammer is used to express the purely outer stresses in the material. The employment of this term is suited, as we shall see later, to the drop impact apparatus and the ram apparatus, although the term does not characterize the fundamental mechanics.

2. Materials destruction through cavitation

Materials testing for strength and corrosion resistance has long been carried out in a systematic manner, but a lack of understanding of the true causes of cavitation and similar water impact stresses has hitherto prevented a systematic investigation of the cavitation attack on various materials as well as their cavitation resistance.

Failure types caused by purely mechanical stresses, such as tension, compression, fatigue, or scouring are different from those caused by cavitation. Figures 3 to 6 give an idea of the type of damage caused by cavitation which, seen in the pure microscopic representation, reminds one of strong chemical corrosion. In America this gave rise to the concept of cavitation corrosion and cavitation erosion. This led to the erroneous view that the primary causes could be considered to be purely electrochemical.

Experiments carried out at the suggestion of Föttinger with chemically resistant materials such as glass, plastics, etc., soon showed that the destruction was caused in the main by mechanical processes and that the electrolytic attacks were secondary and must therefore be of lesser importance. The unique destructive effects, which at times are initiated in extremely short periods, may be classified according to their outward appearances. Depending upon the particular material which is subjected to cavitation, these may be manifested by boils, blisters, pits, sponge-like structures and craters. Occasionally one finds (for instance in glass) evidence of internal rupture and stresses before any destructive effect is noted at the surface (26). Englesson was the first to point to cavitation destruction as being of the nature of a corrosion fatigue failure (19) since, as we shall show in greater detail later, there are always rhythmic stream flows connected with destruction by hydraulic impact. Englesson examined cavitated turbine blades made of various materials--special bronzes, high- and low-alloy steels--and found that their behavior with respect to cavitation stresses is determined by the corrosion fatigue limit. From microscopic examinations it is apparent that there is a deformation of the crystallites at the surface of the pits. Figure 7 shows a cut through the affected region of cast iron in which the graphite laminate has been washed out. Thoma (63) gives a plausible explanation concerning this strain, especially with regard to the strongly grooved condition which originally was smoothly polished. He attributes these appearances mainly to the exploding action in the always present micropores by the impact waves of the liquid.

(According to Allievi

$$\frac{\text{Impact}}{\text{Pressure head}} = \frac{vc}{g}$$

where v is the velocity of the fluid, c is the velocity of sound and g is acceleration due to gravity.)

The pressures reached are insufficient to cause any direct damage; however, they are sufficiently large to bring about localized destruction at the root of the microindentations. Numerous attempts have been made to explain the destruction brought about by cavitation by a multiplication mechanism in the sense used by Ackeret which would give the high pressures necessary to cause this wear in materials. In the case of stellites (non-ferrous alloys) these required pressures are above 10,000 atmospheres. Some of the authors using this explanation were Ackeret (2), Parsons and Cook (43) and especially v. Schwarz and Mantel (55).

Föttinger alluded to attacks of hammer-like pressure impacts on pores and cracks within very small regions. He also thought it possible that as a consequence there might be localized temperature increases.

Nevertheless, the so-called primary process in the destruction of materials remained unknown. This was perhaps due to the techniques employed when testing materials for strength and protection. It is quite

obvious that a different procedure would be required which would permit the evaluation of the types of stresses that accompany the cavitation process.

3. Testing method

The first systematic experiments to determine the wear on materials in the venturi tube by cavitation were carried out by Schröter (51). The evaluation of the material strength was made on a basis of weight loss with respect to time, similar to the method of abrasion or chemical corrosion tests. The results indicate that the weight remains constant at the beginning and that only after a definite period (incubation period) is there a measurable loss of weight which then follows a straight line course. Figure 8 shows the weight loss with respect to time for steels, steel alloys, and cast iron in both the natural and in the annealed state, after being subjected to cavitation in the venturi tube.* This graph shows clearly the incubation period for various materials and also a second characteristic, the rate of weight loss with time (β or $\tan\beta$). Similar results with the curves slightly rounded were obtained by Schröter (52) with his special diffuser, and by v. Schwarz and coworkers (55 and 56) with the drop-impact apparatus.

The rule set up by Schröter, that the weight loss is inversely proportional to the hardness of the material, is valid for high-alloy steels, as was shown by the Karlsruhe tests. For other materials, however, it does not hold. From this it may be gathered that there is no simple relationship between strength of material and the hardness as measured, for example, by the Brinell test. In our discussion, strength of material is understood to be in relation to cavitation resistance. Both Schröter and Föttinger, after testing metals and nonmetals of the most diverse chemical compositions came to the conclusion that the chemical influence upon cavitation cannot be considered as important as the more mechanical stresses acting upon the material. At the suggestion of O. Walchner, Schröter subsequently changed the diffuser so as to have a constricted stream fall upon the test specimen. With such an arrangement Mousson (36) investigated a great number of materials for cavitation resistance in which the volume losses suffered in definite periods were compared. Table 1 gives the results for various sorts of cast iron, after 16 hours of cavitation. The size of the specimen was about 10 x 3 x 0.2 cm.

---

*These test results were obtained by L. Ebert and W. Spannhage with high head orifice at Schwarzenbachwerk. (Tech. High School, Karlsruhe, 1938, unpublished.)

Table 1

Volume loss of cast iron and cast iron alloys through cavitation

Material	Composition in %							Tensile strength		Volume loss after 16 hours mm^3 *)
	C	Mn	Si	Ni	Cr	Cu	Fe	kg/mm^2	lbs/in^2	
Cast iron	3.18	0.50	2.13				Remainder	17.2	24500	696
Cast iron-rough	3.20	0.50	2.30				"	17.2	24500	396
1% Ni-cast iron	2.54	0.76	2.51	1.05			"	38.6	55000	376
5% Ni-cast iron	2.93	0.50	1.36	4.81			"	24.1	34000	269
Ni-Cu cast iron	3.10	1.50	2.00	15.00	1.00	7.00	"	12.4	17600	837
Ni-Cr-Cu " "	2.77	1.00	1.86	14.48	1.88	6.00	"	17.2	24500	247
Ni-Cr-Cu " "	2.95	1.00	1.89	14.36	3.95	6.00	"	24.1	34000	109

*There numbers are merely relative

Micro investigation supplementing macroscopic inspection was introduced by Böttcher (14) in order to study cavitation destruction more closely. Prepared cuts of cavitated materials disclose under strong magnification slippage lines and crack formations which according to Böttcher indicate fatigue in the material. A qualitative evaluation may be obtained by this method of examination inasmuch as the strength of the attack, the type of destruction according to Pagon's classification (42), and the micrographic examination may be affected in the same manner. With the aid of the micrographic procedure, for which purpose polished surfaces are suitable, it is possible to count the individual point of damage from which at the same time the average magnitude of the individual regions may be determined.

Figure 11 shows a brass test specimen which had been subjected to cavitation and in which not only the local destruction but also the exposure of the grains may be plainly seen. At various places there are also plastic deformations which even on plane, smooth surfaces cover an area of about 10^{-6} to 10^{-2} cm^2. This type of deformation may be observed at times after an extremely short interval, a few seconds. In Figure 12 we have the microphotograph of a cavitated brass specimen (Ms 60) which shows a small area of the destruction. If one were to attribute this

damage to purely static-pressure action under normal conditions, then pressures above 9,000 kg/cm^2 (128,000 lbs/sq in) would be required. In this analysis, however, the fact should not be overlooked that alternating stresses of great influence are active which may eventually lead to permanent fractures, especially when there already has been considerable roughening with noticeable loss of weight. In connection with the phenomenon of cavitation, a more thorough knowledge concerning the mechanical stresses which accompany the high deformation velocities (6) would be highly desirable. The plastic deformations shown in Figures 13 and 14 are quite impressive. In Figure 13 we see a macrodeformation of a round cylindrical test body of nonannealed malleable iron which was placed into the high pressure diffuser at the Schwarzenbach plant, while in Figure 14 we see a characteristic center of destruction in a cavitated lead specimen.

4. Resistance to cavitation and the mechanical properties of materials

In the attempt to classify the cavitation effects, one of the first difficulties arises when we compare the loss of volume through wear with the physical properties of the materials. The metallic materials investigated by Mousson (36) were low- and high-alloy steels, stainless steels, surface treated steels, aluminum alloys, and nonferrous alloys such as bronzes, brasses, and stellite. The comparable measure of the quality of the test bodies was the volume loss after 16 hours of cavitation. In the sense of the so-called erosion which bears a close relationship to the hardness of the test material, Schröter arrived at a simple working theory which made the wear on the material inversely proportional to its hardness as measured for example by the Brinell test.* It appears logical at first that the cavitation stresses are produced by small liquid pistons acting on many localized points. The results obtained by Mousson and also those obtained at Karlsruhe show that the relationship $H_B \Delta V = k$ is not invariable, even within a special group of metallic materials. This is shown quite plainly in the graphic representations of Figure 8 in which the weight loss with respect to time is given. For cast iron the increase in hardness is accompanied by a disproportionate increase in wear, for carbon steel there is no marked change with increased hardness, while for highly alloyed steels there is considerable improvement to cavitation resistance with increased hardness. The relationship, however, holds true for the same material which has been subjected to various heat treatments. For example, Mousson found after 16 hours cavitation in the case of a stainless steel (12.25% Cr, 0.12% C, 0.45% Mn, 0.025% P, 0.40% Si, and 0.025% S) the following:

Hardness H_B	142 kg mm^2;	volume loss 46.7 mm^3
	219	20.3
	285	8.3
	401	3.5

*In Vater's drop impact tests the volume loss diminished with an increase in hardness. Austentite steels, however, formed an exception.

This seems to indicate that individual inner structural properties of the material such as the crystal grain, grain adhesion, separation, etc., may be considered as having some bearing upon cavitation resistance rather than the collective outer properties.* On the other hand there are materials with but little difference in their chemical composition and with about the same degree of hardness which, nevertheless, display a marked difference toward cavitation. A molybdenum steel (C 0.27%, Mn 0.75%, Mo 0.52%) with a Brinell hardness $H_B = 192$ kg/mm^2 has a 35 percent higher loss through cavitation wear than a Ni-Cr-Mo steel (C 0.28%, Mn 0.65%, Ni 1.37%, Cr 0.60%, Mo 0.25%) with $H_B = 179$ kg/mm^2, both having about the same tensile strength, elastic limit, ductility, and stretch at break. It is, therefore, not surprising that no relationship can be established between tensile strength or elastic limit and cavitation resistance except for the special case of a certain metal which has undergone a different heat treatment. This lack of relationship holds also for maximum ductility or for elongation at break. Even with a respect to the static energy there is no intimate connection. A Si-Ni-Cr-Cu steel with the following data: $H_B = 166$ kg/mm^2; tensile strength = 53 kg/mm^2; elongation at break = 17 percent is more resistant to cavitation than a tempered high alloy steel (Cr-V-W) with a Brinell hardness $H_B = 415$ kg/mm^2, tensile strength = 152 kg/mm^2, and elongation at break = 41 percent. The fact that there is a great diversity in the requirements for cavitation resistance is quite apparent. Even within similar groups of materials the results show volume losses which may be twice and sometimes even three times as large. The strength to withstand cavitation is, therefore, much more characteristic than the ordinary strength properties. The cause for this lies evidently in the peculiar type of the stressing process which must be a coupling phenomenon.

The larger the number of damaged places present or engendered, the more areas subject to the primary process.** This leads to an exponential dependency whereby the quality of the various materials may be strongly differentiated. Mousson found a 16-hour loss through wear of 3.7 mm^3 in a stainless steel with about 18-percent chromium ($H_B = 182$ kg/mm^2, tensile strength = 84 kg/mm^2, elongation at break = 37%) while for one with about 12-percent chromium ($H_B = 178$ kg/mm^2, tensile strength = 60 kg/mm^2, stretch at break = 74%) the loss was 24 times as much. Since a simple proportional relationship does not adequately describe the curve, a more precise analysis is possible only when the total loss of weight with respect to time is known. In order to characterize this curve, two terms are required, provided that the interval is not too distant from the incubation period. One difficulty arises in standardizing such a testing procedure when there is much loss through wear; through strong macrochanges of the surface the stream flow may be retarded. On the other hand the method of counting the points of damage under microscopic examination is very time consuming when the cavitation attack is weak. It is therefore important to use relatively small, light test bodies in order to determine exact weight losses, even when there is but little cavitation.

---

*According to v. Schwarz and Mantel a high degree of hardness and cold forming properties are conducive to cavitation resistance.

**By primary process is meant that mechanism which is active at the collapse of the vapor pocket which is located at the surface of the material.

For purposes of comparison, Schumb, Peters, and Milligan (54) carried out sandblast tests in which the effect on various materials was investigated. While the wear produced by this method is not analogous to that caused by cavitation, there is a certain similarity in the destructive process. It is clear that the familiar properties such as Brinell hardness and tensile strength determine the resistance of a material to sandblasts.

The characteristic signs of the cavitation effects can be found in all related water impact destructions, not only when examined macroscopically but also when viewed microscopically. Even before Schröter conducted his experiments with the modified diffuser, in which the jet of water impinged directly upon the test plate, Honegger (27), de Haller (24) and later v. Schwarz and Mantel (55) employed the drop-impact apparatus in which the test specimen which has been attached to a rotating carrier cuts through a jet of water of about 6 to 8 mm cross section with a high velocity (80 m/sec, 265 ft/sec or more). The type of damage observed and also the weight loss curves resemble those obtained in the venturi tube (34). The same drop-impact procedure was followed by Vater (65 and 66) and he, like Englesson, came to the conclusion that cavitation resistance depended upon the strength of the material. In test specimens which were artificially pitted typical signs of permanent failure could be observed. It was possible to obtain characteristic curves for various materials somewhat like the Wöhler curves (in this case velocity with respect to the number of impacts). Figure 15 shows these for a number of steels. In a spray-impact test on copper which lasted for only one-thirtieth of a second, Vater (68), on the other hand, found dents with a depth of 0.07 mm and a diameter of 0.2 mm. It is quite clear that in this case the stress was not of any appreciable duration.*

Ackeret and de Haller (5) developed an apparatus which also causes typical cavitation. In this arrangement a movable piston strikes a confined liquid which covers the test specimen, with a frequency of 16 cycles per second. Figure 16 shows the groove in a grey cast-iron specimen before and after 60,000 impacts. In this the graphite layers are entirely washed out. Many of these destructions are considered to be the effects of genuine groove actions; there are, however, cases in which purposely made microgrooves are again rolled together. A fine example of this is shown in Figure 17.

The unique behavior of materials towards cavitation has made it impossible to determine the required pressures which bring about the plastic deformations through static or dynamic actions. This is of course not surprising. Using quartz crystals, both de Haller and E. Spannhake have attempted, unsuccessfully, to attain higher pressures through a multiple coupling mechanism in which the pressures are measured oscillographically. Also in the impact apparatus of Ackeret and de Haller, there are no pressures higher than the hydraulic pressure. However, one must

---

*According to the tests carried out by Vater (67) the cavitation attack in the drop-impact apparatus is a function not only of the velocity of the jet, but also of its cross-sectional area.

remember that the destructive action of the so-called primary process is generally confined to an infinitesimal region, which accounts for the difficulty in making the measurements.

We shall, incidentally, mention here of another experiment in which characteristic cavitation damage is brought about. If an air bubble resting on an immersed wire is compressed by a pressure wave which is induced in the liquid, then there will be seen evidence of cavitation which is peculiar to water impact damage (48) at the place where the bubble had been.

5. The periodicity in cavitation

The influence which the number of individual attacks per unit time has upon the intensity of the cavitation is self-evident. Cavitation affects are always specially pronounced in those regions where periodic action takes place. In the impact apparatus they have a frequency of 16 cycles per second and in the venturi tube frequencies of several hundred cycles per second are not uncommon. Cavitation attacks of great intensity were obtained with oscillators in which the frequencies run in the thousands. The periods in the drop-impact apparatus is governed by the revolution of the specimen holder. It is certain that in all the methods used, higher hormonics of great intensities are at times induced; this assumption is suggested especially in cavitation in the venturi tube where it is impossible to analyze a wave spectrum within a confined range.

The problem of cavitation is resolved into a predominantly hydrodynamic question considering the motion of the fluid particles as well as the vapor or gas bubbles and into the study of the materials destruction itself. In this manner the subject is considered from two angles, cavitation attack and cavitation resistance. From oscillographic film exposures in the venturi tube experiment, the rhythmic motion of the vapor bubbles, their collapse, disappearance, and recreation can be observed to be in the same periodic interval as the detachment of the water column from the narrowest cross section of the tube. In the oscillator the same course is followed, strong bubble formation, vaporization and recondensation; also high and especially large accelerations in the motion of the fluid enter into the picture. Mueller (37) in his "Slow motion pictures of a cavitating airfoil," definitely proved the existence of collapsing vapor bubbles. The calculated impact times are somewhere near 0.0033 seconds.

II. GAINES' OSCILLATOR

6. Arrangement

In 1932, a paper by Gaines (22) reported an apparatus which was able to induce strong and characteristic cavitation action.* It had the advantage that it required but little power and that it could be conveniently

*Fottinger also, as early as 1932, called attention to cavitation by means of ultrasonic waves.

manipulated (30 and 62). As used here, advantage is taken of the magnetostriction of a nickel rod in a changing field. The phenomenon of magnetostriction, discovered by Joule, was first used, especially by Pierce, as a sonic oscillator. A self-exciting electron tube was connected with the rod which served as the wave transmitter. In their varied arrangements, these oscillators have in recent times found numerous applications in the field of ultrasonics. (See reference (10).) Besides pure nickel, there are nickel alloys, invar, and monel metal with a trace of iron or silica which are suitable for this purpose. In order to obtain the required high frequencies (100 kilocycles and higher), Pierce, Kallmayer, and other investigators have used special types of rods. In Gaines' arrangement a changing magnetic field of some 9 kilocycles is attained. The nickel tube about 25 cm long, excited longitudinally, has one end oscillating in the liquid. A 250-watt transmitting valve acts in reverse (Rückkopplung) through the magnetostriction effect. Figure 18 shows the fundamental arrangement. Our own experiments were carried out with an apparatus that had some improved features; it is seen in Figure 19, together with the measuring microscope. The changing field originates in the electric oscillating circuit and is formed by the oscillator coil L, and the condensers C_1 and C_2 (Figure 18). Synchronization is effected when the oscillating circuit works on a frequency of 9 kilocycles which corresponds to a rod length (tube length) of 26.2 cm. ($L = \frac{1}{2} f\sqrt{\frac{E}{\rho}}$, where L is the tube length, f the frequency, E the elastic modulus, and ρ the density of the material of the tube.) A 400-watt transmitter tube forms a regulating mechanism free of inertia. A direct-current generator supplied directly the required voltage of from 2,000 to 3,000 volts. If one is not available, then the direct-current is obtained through a high-voltage transformer T connected with two mercury vapor rectifiers for which T_2 is the necessary heat transformer. This is shown schematically in Figure 18. The pulsating direct-current is then evened out through the condensers C_3 and the valves L_3. Transformer T_3 furnishes the heat for the transmitting valve. The induced voltage change in coil L_2 furnishes the regulating impulse to the grid. With the aid of resistance R_1, the most favorable point within the straight part of the characteristic curve for the tube may be obtained. In order to have larger amplitudes without doubling the frequency, it is advantageous to premagnetize the yoke by a direct-current field while the directanode current is permitted to flow across the oscillating coil. The yoke-shaped oscillator frame we used is schematically given in Figure 20. The knife-edged clamps for the rod are here replaced by a sphere-like clamping shell which permitted a rapid exchange of the test specimen without throwing the oscillator rod out of adjustment.

Between the oscillator coil and the clamping shell there is a protecting ring about 10 mm wide to prevent the flow of stray currents from the lower part of the coil to the tube clamp, partly avoiding the heating of the clamp.

For a satisfactory performance adequate cooling is necessary. The nickel tube as well as the oscillator coil became exceedingly warm during

operation. To dissipate some of this heat, the oscillator tube is split along that part which is taken up by the coils. This permits the passage of air currents. Water cooling was occasionally tried by simply closing the tube with adhesive tape. Permitting the cold water to enter at the top and syphoning it from the bottom makes likely a water column of variable height which disturbs the steadiness of the frequency. In order to get around this difficulty, Gaines fastened his test body at the upper end of the oscillating tube. The water forced into the tube from below did not change the resonance. This necessitated, however, packing the tube against the loss of the liquid used in the experiment. It was found that a stable frequency could be maintained by boring outlet holes directly above the lower end of the tube through which the cooling water was allowed to escape. In that case the inner face of the test bodies had a conical shape. (See Figure 22.)

An effective cooling was obtained by means of dry ice. At 5-minute intervals little pieces were dropped into the tube. The carbonic acid vapors escaping through the slit of the tube cooled the oscillator coil. No irregularities in the frequency were observed.

The shape of the test bodies and the manner of their attachment to the oscillating tube presented a problem. Its solution depended on the determination of the influence which the weight of the specimen had upon the frequency of the oscillator tube. Figure 21 shows this influence graphically. The shapes of some of the test bodies used can be seen in Figure 22; as far as possible they were made of light metals. The test bodies used in the weight-loss experiments were made especially small and fastened onto the tube by an aluminum bushing. We noted that a faulty attachment of the test specimens at times caused irregularities in the frequency and that test bodies which are cracked within were out of harmony with the rod frequency due to strong damping. The amplitude is measured indirectly by electrical means. A coil of 100 turns at the free end of the oscillating tube induces voltages that are indicative of the amplitudes. After a microscopic calibration for definite amplitudes (from 0.01 to about 0.09 mm), a precise determination is possible. Protection is provided against the part of the apparatus carrying high voltage.

7. Cavitation produced by ultrasonic oscillator

The experiments by Gaines (22) and later those by Schumb, Peters, and Milligan (54) as well as those by Kerr (32) already pointed to the correspondence between the type of destruction produced by the oscillator and the cavitation damage appearing in the venturi tube. The curves in Figure 23, taken from the work by Kerr, show the weight-loss relationship in mg for periods to 120 minutes for brass, cast iron, cold-rolled steel, and stainless steel. Kerr also compared the resistance to cavitation for various metals which had been subjected to cavitation in the high frequency oscillator and also in the venturi tube.

H. Peters and B. G. Rightmire* carried out experiments to establish the relationship of cavitation intensity to static pressure for various water temperatures, using brass test specimens. The results of their investigation are shown in Figure 24. For atmospheric pressure $p = 1$ atmosphere the curve giving the loss of weight shows a maximum between 55° and 70° C for water. Near the boiling point any attack by cavitation vanishes.

For a pressure $p = 2.4$ atmospheres there is some shifting for the maximum and for $p = 3.1$ atmospheres, the maximum lies obviously beyond 100° C. The behavior at the pressure $p = 2.0$ atmospheres is entirely unexplainable. From these tests the authors obtained expressions for V_r and p_r, where V_r is equal to a reduced volume loss, while p_r corresponds to a reduced absolute pressure:

$$V_r = \frac{\Delta V}{fa^3} \qquad \text{and} \qquad p_r = \frac{p - p_s}{\rho (fa)^2};$$

ΔV is the volume loss for each vibration per volume a^3, where a is the amplitude; ρ is the density of the liquid. In connection with this, there exists the functional relationship $V_r = F(p_r)$. The reduced volume loss is small for $p_r = 0$ or for very large values of p_r; between these, there is the greatest cavitation destruction.

Of the various testing arrangments--venturi tube, drop-impact apparatus, and oscillator--the oscillator requires considerably less energy than the others. There is a further advantage; cavitation is brought about very quickly and consequently more observations are possible for the study of the cavitation process. From the few experiments which have been made it is quite evident that the properties of the liquid such as vapor pressure and the absorbed gas play a considerable part in the process. The question of the vapor bubble formation, which always arises in connection with the phenomenon of cavitation, may be studied here by direct observation. Any desired liquid may be employed; it is possible to change the vapor pressure, surface tension and viscosity to find out the nature of the primary process of the cavitation attack and thereby arrive at some valid general rules which will aid in the selection of a materials testing procedure. Furthermore, it permits an observation of the material during the so-called incubation period and after the completion of the experiment not only the test specimen but also any detached pieces may be separately examined. To arrive at a technically valid standard concerning cavitation resistance, one must ascertain the degree of the mechanical and chemical influence, whether constant stresses play a role or whether there is within the crystal itself a damping of the vibrating parts of sufficient magnitude to have any effect.

---

*Private report to Prof. W. Spannhake.

8. Methods of measurement and general observations

Although valuable information is obtained by a macroscopic examination of test specimens which had been exposed to cavitation and which are ground and polished, a microscopic investigation as introduced by Englesson (19) and Böttcher (14) affords much additional valuable data. Microstructural investigations carried out with the aid of X-ray interferometers should give information concerning changes in cleavage of the crystal grains or the change in bondage as the result of cavitation. The superimposed forced vibration causes the test specimen to form nodal lines and vibration bulges which naturally depend upon the shape of the specimen and to a lesser extent upon the manner in which it is clamped. Therefore, the proper preparation of the test specimen is of importance. Figure 25, from Gaines, shows such lines, and Figure 26 illustrates a kidney-shaped test body in which the major damage occurred upon the curved portion.* In some very brittle materials we observed that the test specimen vibrates but little or not at all, and consequently there is no cavitation damage when there are internal fractures to begin with or if such be caused by the vibration. In this case we deal with typical damping phenomena of vibrating materials which are used in modern materials testing for the detection of haircracks, blowholes, and other defects.

Much care must be exercised in the preparation of the test specimens with respect to shape, clamping, and weight in order to have a standardized testing procedure so that proper comparisons are possible. Hitherto the loss of volume has served as a measure of the cavitation intensity which is determined by the difference in weight. Another successful method by which cavitation attacks may be evaluated, especially those of small intensity, is by counting and measuring the individual points of damage in the microscope. Although time consuming, this procedure is better than that of the volume-loss method. In aluminum, for example, there are crater-like formations which are due to cavitation (Figure 27). Such materials show at times but little loss of weight, which might lead to the belief that there is no cavitation attack and that the material has a high cavitation resistance. In tests with aluminum bodies in which large amplitudes were used, a regular atomization was observed, whereby the particles remaining in suspension were quite uniform and of the order of 10^{-5} cm. In general, however, the cavitation effects are of a pit-like nature so that the loss of volume is a measure of the cavitation damage. When the operation periods are prolonged there is, without doubt, a change in the vibratory condition, due to the loss in volume. This might explain why there is sometimes a diminishing loss in weight after there has been a very considerable destruction of the material.

The quantitative evaluation of the weight loss with respect to time for a magnesium test body which had been subjected to cavitation in water is represented in Figure 28. This curve also permits a separation into two

---

*According to Beuthe (11) the vapor pocket formation takes place in the vibrational crests and not in the nodal lines.

intervals, that at the beginning when there is no noticeable loss in weight (incubation period) and that part of the curve in which the weight loss follows very much a straight-line course. In the oscillator experiment we found the break in the volume loss (weight loss) to be quite abrupt; this was also characteristic of the recently published time-weight loss curves by Kerr (Figure 23).

In the oscillator tests, the incubation period is a matter of minutes. If in our apparatus we roughly figure on a 10-minute period for iron and steels then we have up to the beginning of actual destruction about 6×10^6 impacts. In the venturi tube at the Schwarzenbach plant the time required was about 8 hours. The jet frequency computed by E. Spannhake's formula equals about 300 cycles per second, indicating that there are from 8×10^6 to 9×10^6 impacts. This shows a remarkable correspondence between these entirely different testing procedures, the venturi tube and the high frequency oscillator. In the drop-impact experiments carried out by v. Schwarz and coworkers the first strong attacks on steels were noted after 1×10^6 to 3×10^6 impacts.

A large number of tests are necessary since there are considerable deviations of weight losses, especially with larger amplitudes. In Figure 29 the weight losses in aluminum specimens subjected to cavitation in water at room temperature are plotted as a function of the amplitude. This shows not only that the curve rises rapidly when the induced voltage is greater than 30V (corresponding to an amplitude of 0.05 mm) but also that average errors amounting to 60 percent are possible. On first thought, this appears to limit the usefulness of the procedure somewhat, but we are reassured when we consider that the deviations of cavitation resistance for individual materials are no greater than those encountered in testing for tensile strength, Brinell hardness, or other mechanical properties.

For purposes of comparison we give the relative ratios of the volume loss for several materials for a given time lying beyond the maximum incubation period:

Alluminum alloys	Cast iron	Tempered steel (0.33% C)	Drawn Cr-Mo-steel (1.1% Cr; 0.5% Mo; 1.37% Mn)
≈1,000	≈100	≈10	1

III. CAVITATION ATTACK

9. The vapor pocket formation at the boundary surface

When pressure regions exist, for example, in a venturi tube, which approach the pressures of the water vapor and when the hollow pockets formed thereby collapse, it is certain that damage will result. Our study deals with vapor formation and recondensation, the same as in bubble and foam formation.

As is seen from Figure 20, the test specimen fastened to an oscillator tube is immersed into the liquid to a depth of about 1 mm. If the testing period extends over any length of time, the immersion depth needs to be watched as there is accelerated vaporization.

What are the steps through which cavitation proceeds in the oscillator and how does the damage appear to the eye? The primary purpose of this experiment was to find a direct connection between vapor pocket formation and cavitation erosion. In the oscillator the vapor bubbles and their motion could be followed quite easily. The photography of the vapor pocket formation was effected with the aid of a reflecting mirror, the container holding the liquid being a very flat bowl. Figures 30 to 34 give views from below against the piston surface of bubble formations for various liquids such as benzol, glycerin, paraffin oil, and water at room temperature and at 80° C. In order to determine the direct connection between the distance separating the location of pocket formation and of the cavitation attack, the camera exposures were made from below which in effect gave a top view. Steel test specimens were found very suitable for this purpose, their high cavitation resistance preventing noticeably the retroaction upon the vapor formation and recondensation during the time of camera exposure. This is due to the roughened and stressed surface of the test sample. Figures 35 and 36 are exposures of tests carried out with two different frequencies; they show clearly that foam formation increases with higher frequencies. The vapor bubbles tend to collect along separated lines and in the case of low water temperatures cause the greatest damage in the center of the test piece, as we will show later. The light surface in the center of Figures 30 and 36 represents a comparatively large vapor bubble of about 1/2 mm in diameter. Whether this is the same bubble or whether it is an ever newly created bubble by the rhythmic frequency cannot be observed visually. As yet it has not been possible to film cinematographically anything with a frequency as large as that of the oscillator. However, we know that the larger bubble has "a definite life span." The evidence for this is the ever new formation of bubbles of about the same diameter which remain visible for awhile before they collapse. Almost immediately after the collapse of the first bubbles a microscopic investigation shows strong materials attack at the point of collapse. With water at higher temperatures the diameter of the bubbles is smaller.

A comparison of Figure 30 with Figure 31 shows, furthermore, that in the case of hot water the bubbles spread from the center over the entire upper surface. They are here about the same size as those formed in benzol or glycerin. In glycerin they form a honeycombed closed space beneath the test specimen. The development of these after one-fourth and one-half second are shown in Figures 37a and 37b. In contrast to the light surface in Figures 30 and 36 there is no large single bubble. Within this honeycombed space a sort of bubble ray (Bläschenstrahl) is always in motion beginning at the midpoint of the test piece, going into the fluid and returning laterally to the test specimen. Paraffin oil as a cavitation medium gives rise to a similar phenomenon. The difference in cavitation erosion in various liquids comes from the distribution of the points of attack and in the strength, depending upon the stream flow of the liquid. In the case of slightly viscous fluids, such as water and benzol, a

well-defined bubble ray originates at the test piece but extends to the wall of the vessel where numerous bubbles are deposited. It is clear that such properties as surface tension, vapor pressure, and viscosity, which in turn depend upon temperature and pressure, determine the mechanism of the bubble formation and the collapse of the fast holding vapor or gas bubbles.

10. Damage brought about in water and aqueous solutions

In their cavitation investigations, Schumb, Peters, and Milligan (54) used methyl alcohol and carbon tetrachloride besides water with the temperatures of the liquids as the variable. Their results show that in the case of water the attack reaches a maximum at about 50° C; it becomes negligible as it approaches the boiling point. A similar behavior was noted also with carbon tetrachloride where the maximum value is from 25° to 30° C. In methyl alcohol, however, there was a steady decrease of cavitation action with rising temperatures. The authors then mentioned the possible connection between the degree of destruction and the outer pressure, or the vapor pressures, respectively, of the liquids. However, they believed that the ratio of the vapor pressure to the outer pressure, $\frac{p_s}{p}$, was not the most essential factor. (They found the maximum value at $\frac{p_s}{p} \approx \frac{1}{4}$.) The writers ascribed an important role to the gas content. For example, aluminum experienced a tenfold destruction in partial gas-free methyl alcohol over that in gas-saturated methyl alcohol. Specimens tested in water at room temperature always show the first and greatest evidence of attack in a circular area about the center of the test piece regardless of the type of material used. Figures 38 to 47 show the destruction of aluminum in water with temperatures between 10° and 100° C.

There is remarkable correspondence between the widening of the foam formation at the surface and the region of destruction with an increase in temperature. At 60° C the foam formation is a ring about the midpoint which is hardly attacked. At 70° C the much weakened attack occurs within a broader concentric ring and at 90° C the effect of any strength is lost. If we recall the corresponding pictures of the stream formation we may see that the damage is somewhat a replica of the vapor bubble formation. If the vapor bubbles originate and vibrate mainly about the center, then it is also there that the strongest attack takes place. We, therefore, deduct the type of stream flow and cavitation attack from the distribution and kind of damage to the test piece.

For the precise temperature determination one element of a thermocouple was fastened to a hole in the locknut. The average of the temperatures taken at the locknut and the bath, taken with an ordinary thermometer, was considered as the true temperature at the boundary surface. In some of the tests, marked by excessive temperature fluctuations, the cooling of the vibrating tube was found insufficient, and their results were not included in the tabulation. The comprehensive test series represented by Figures 38 to 47 show in characteristic steps the dependency upon the temperature at

atmospheric pressure. At first the damage increases with rising temperatures, the damage, however, being confined to the center of the test piece. At 60° to 70° C the inner seat of destruction is widened until finally it takes on a ring-like form. The area of attack is more and more toward the sides, the intensity of the damage becoming visibly smaller. At 90° C there is but little evidence of cavitation and at the boiling point there is none. The concentrated attack is greater at low than at high temperatures which may be due to the size of the vapor pocket; but the total area of attack increases with an increase in temperature (stronger bubble formation).

The disappearance of any damaging action as the boiling point is reached proves that cavitation is tied up with the dual phase condition. The number of vapor bubbles is evidently connected with the height of the vapor pressure in such a way that the bubble formation is stronger when the vapor pressure is high. Aside of the surface tension, the instability of a bubble is dependent upon the difference between the outside pressure and the vapor pressure.*

With little or no bubble formation, resulting from diminishing fluid cohesion, there is no damaging action. This qualitative view of the mechanism of cavitation leads to the assumption that there are two participating factors, namely, the number and the stability of the bubbles. It can easily be seen why there is a maximum value for cavitation erosion between 0° and 100° C, as is shown in the graph of Figure 24, the pressure being atmospheric.

The quantitative effect of cavitation on a magnesium test specimen was determined by the weight loss. The graph in Figure 48 gives this in proportion to the temperature of the water. It might be stated that this temperature dependency is valid for all the materials examined, regardless of the type and mode of preparation. Tests were carried out with brass, cadmium, steel, magnesium, plexiglass, and other materials.

Through the roughening of the surface by cavitation, the vaporization mechanism is somewhat altered, depending on whether the walls are smooth or have micropoints, edges, or pits. The manner of foam formation too gives rise to smaller changes with time.

The solutions used as test mediums were dilute hydrochloric acid (1/100 N), potassium hydroxide (1/100 N), salt solutions of various concentrations, and 30-percent hydrogen peroxide. There is but little difference in the foam and bubble formation from that observed in distilled water or common tap water. As is known, the vapor pressures of diluted electrolytes vary but little from those of the pure solvents. Consequently, one can expect a similar bubble formation and also a similar type of cavitation erosion. (See Figures 49, 50, and 51.) A marked chemical influence

---

*For static equilibrium of a bubble in liquid the following expression is valid: $p_i \cong (\frac{2\sigma}{r}) + p$, where p_i is the inner pressure, σ the surface tension, r the bubble radius, and p the outer pressure.

expected with the various solutions did not materialize when pure aluminum specimens were used. Any possible chemical corrosion damage was by far overshadowed by the much greater cavitation destruction. We shall see later, however, the role which the chemical behavior plays. The total weight loss was here, also, a maximum at about 50° C with a test period of 10 minutes. The evidence that the strength of the attack is a function of the temperature is repeatedly brought out; this leads to the conclusion that in the main the attack by cavitation is somehow dependent upon the physical condition of the vaporized liquid.

11. Damage brought about in organic liquids

To determine the influence of the physical condition of the medium upon the cavitation of materials we employed liquids which differ markedly from aqueous solutions as to vapor pressure, surface tension, and viscosity. Since pure aluminum shows cavitation effects in a reasonable time we used it for test purposes.

The attacks by benzin, benzol (octane-nonane mixture), and ethyl ether at room temperature are pictured in Figures 52, 53, and 54. From these the remarkable correspondence with water at 20°, 60°, and 90° C is seen, perhaps not in the strength of the attack but in the area affected. The vapor pressures for water at these temperatures are 17, 150, and 525 mm, respectively. At 26° C, which was the average testing temperature, the vapor pressures for n-octane, benzol, and ethyl ether are about 16, 100, and 500 mm, respectively. It appears, therefore, that the type and strength of the cavitation is determined by the vapor pressure. In the case of ether no cavitation damage could be noted even after a long exposure, only a slight effect being visible through the microscope. This resembles the cavitation attack of water near the boiling point.

The tests were extended to include alcohols and benzines whose boiling points lie between 60° and 136° C. Figure 55 shows the results of a 10-minute exposure to cavitation of the aluminum specimens for the same oscillating frequency in cyclohexane, n-heptane, n-octane, methyl, ethyl, and iso-amyl alcohol. Along the abscissa we have instead of temperatures the vapor pressures in mm Hg. Two facts are apparent; that there is almost complete correspondence in the cavitation attacks for various liquids with equal vapor pressure and that the attacks disappear as the liquid approaches the boiling point. Consequently the hydrodynamic state is only indirectly dependent upon the temperature. In the liquids used the surface tension in the vicinity of the boiling point ranged between 12 and 18 dynes/cm. The disappearance of the cavitation attack at the boiling point furnishes proof that the phenomenon of cavitation is primarily connected with the dual phase, liquid-vapor; a pure vapor cavitation is impossible since the necessary mechanism for the formation and the collapse of the bubble is absent. To be sure, the bubble formation near the boiling point ($p_s \approx p$) is greatly enhanced by the accelerated vaporization due to cavitation, yet these vapor bubbles are unstable and lose their ability to hold fast and to vibrate, they simply puff off. Through the increased vaporization, these bubbles and the foam formation are forced away from the center. Since on one hand

we have stable vibrations in the center of the test specimen and on the other we have an impelling centrifugal force with increased vaporization, it is clear that in this case the most propitious place for a stable vibrating condition of the bubble foam is somewhere away from the center. This explains the ring-like destruction, whose position is determined partly by the oscillating frequency and partly by the vapor pressure. An important experiment on this phenomenon revealed the remarkable stability of the vibrating gas bubbles. With the aid of a piece of wire a bubble about 1/2 mm in diameter was moved back and forth over the surface of the test specimen. The resultant damage covered a considerably enlarged area.

The primary reaction is a function of the mechanism of the bubble formation and of the vibration of the bubbles. To what extent the formation is dependent upon the magnitude of the surface tension and how much type of motion is related to such secondary conditions as viscosity, are problems which require a separate treatment. In addition the various mechanisms should be studied independently; in other words, when there is a large number of active bubbles to what extent is their stability and their ability to hold fast governed by the vapor pressure or by the outer pressure, respectively? It appears that the surface tension exerts less influence upon the area of attack than upon the size of the bubbles as seen on comparing the damage done in water and benzol. In the former the strength of the attack is greater; however, the affected area in each case is much the same. We point to this, since the primary reaction of water is in itself much stronger. The surface tensions of the two liquids are 72 and 28 dynes/cm, respectively, while their viscosities are not too different, their ratio being 10 to 7.

However, if one examines closely an aluminum test piece cavitated in castor oil, which has a viscosity so much greater than that of water, one must assume that the development of larger bubbles is hindered by the strongly retarded flow. In glycerin too the slowly moving bubble cloud is in a different hydrodynamic condition than the bubbles in an easily flowing liquid; the bubble stream is steered directly through the liquid. The damage shows most where the bubbles adhere the longest which in this case is at some distance from the center of the test piece (see Figure 37). Castor oil has a viscosity some 1,000 times that of water; in such fluids the stationary bubble cloud has a stream flow somewhat perpendicular to the center, returning by a path tangentially to the upper surface which explains the length of time the cloud remains between the center and the edge. In the case of mercury acting on magnesium the behavior is naturally much different, the magnesium suffering a loss of 1/2 cm^3 in almost half a second through exceptionally rapid amalgamation.

On the basis of these first considerations we assume that by changing the temperature and pressure of the various mediums we may arrive at a separate treatment of the primary reaction on one hand and its concomitant conditions on the other.

12. Degree of damage caused by oscillating vapor bubbles

We can see from the foregoing that the damage is a direct reflection of the condition of flow or the formation of the bubbles and that the primary reaction is tied up with the behavior and the properties of the momentarily attached bubbles. Since the surface tension is decisive as to the stability and the viscosity as well as to the motion of the bubble, the determination of the causes of cavitation resolves itself into the following investigations: vapor pressure (p_s), outer pressure (p), surface tension (σ), and viscosity (η). The question naturally arises whether any further evidence could be called upon before the acceptance of a mechanism of the collapsing or compressing bubbles which accompany the damage. On observing the motion of the liquid during cavitation, one may note a movement of the bubbles across the surface of the test specimen, which at times becomes quite jumpy. This motion is seen especially in highly viscous liquids, but if the amplitude of the vibration is small it can also be found in less viscous liquids such as water. With a high-speed movie camera, we measured the velocities of these bubblets, whose motion is mainly away from the center, and noted a speed of a few centimeters per second. Previously, Gaines took pictures of such a bubble trail in which the vapor pocket vibrated "in resonance," finding the relationship

$$d = \frac{v}{\pi f}$$

to hold true. Here, d is the bubble diameter, v the velocity of the bubble core (Blasenverkleinerung), and f is the frequency. We were successful in observing microcavitation on ground and polished test specimens which was directly attributable to these vibrating vapor bubbles. Figures 56 to 61 show enlargements of this microdamage on metals and nonmetals. These unique damage paths can be explained by assuming that such a vapor bubble travels along the surface of the test piece with a definite velocity, expanding and contracting in unison with the oscillator, so that by every collapse a localized destructive effect takes place. The tangential velocity may, therefore, be determined from the distance between two neighboring dents when it is considered that this distance Δs represents the path of one bubble during one vibration period. We then have

$$v_t = \overline{\Delta s}\, f,$$

where v_t is the velocity of the bubble between the surface limits and f is the frequency of the oscillator. If we measure the average Δs in Figure 57 as 0.0003 cm (enlargement is 380 times), we obtain a velocity v_t of about 3 cm/sec ($f \doteq 10{,}000$ Hz or 10 kilocycles), which is in harmony with the observed bubble velocities. Similar paths of destruction were observed on specimens cavitated in the venturi tube at the Schwarzenbachwerk (Figure 62).

13. The relationship of the cavitation attack to pressure and temperature

The results obtained in the previously mentioned experiments, carried out with hyperatmospheric pressures under various temperatures, can be explained in a simple manner by merely extending our assumption and by comparing these results with those at low temperatures under standard pressure. Figures 63a to 63c from the work of Peters and Rightmire support our assumption as it concerns the strength and the distribution of the cavitation attack. A specimen cavitated at 100° C at an excess pressure of 1 atmosphere shows quite similar effects to one attacked at from 60° to 70° C at standard pressure. Also the effect at 80° C and 1-atmosphere excess pressure corresponds to that at room temperature and normal pressure.

In order to test our view that apparently there is only the mutual dependency of outer pressure and vapor pressure we carried out cavitation experiments in water at room temperature (25° to 27° C) with outer pressures below 760 mm Hg. Figure 64 illustrates the experimental arrangements. A glass vessel to which an exhaust pump can be attached is fastened to the oscillating tube and made airtight with a rubber hose. Figure 65 shows the cavitation effect on aluminum test specimen with the vapor pressure $p_s = 30$ mm Hg and the outer pressures p at 30, 250, 380, 500, 550, 600, 650, and 760 mm Hg. For the purpose of comparison, tests at normal atmospheric pressure were also carried out to see if any differences could be detected due to the fastened oscillator tube. As had been expected, no damage could be observed on the test piece when the outer pressure equalled 30 mm Hg, even after several hours of testing. The cavitation damage at one-half atmosphere corresponded somewhat to that between 70° and 80° C at standard pressure. Notice should be taken of the difference in exposure time between these tests and those represented by the series of Figures 38 to 47--10 minutes as against 1 minute with, however, higher amplitudes. The boiling points of water at 1/2, 1, and 2 atmospheres are 80°, 100°, and 119.6° C. One can readily see, therefore, that for the cavitation mechanism the difference $p - p_s$ plays a fairly deciding role. The volume loss for $p - p_s = 350$ mm Hg is considerably less than for $p - p_s = 570$, 620, and 730 mm Hg. The maximum value (reached when $p_s \approx \frac{3}{4}$ atmosphere or 570 mm Hg and outer pressure p equalled 1 atmosphere) is somewhat less impressive here. In connection with these findings, a simple explanation can be given to the results obtained by Peters and Rightmire in their cavitation experiments with excess outer pressure; since the dual phase with excess pressure extends from 1° to 120° C, there is still a considerable difference at 90° or 100° C between p and p_s, necessary for cavitation action. On the basis of the rule that when $p - p_s = 0$ there is no cavitation damage, an explanation can be given why the destruction does not take place in the area of the venturi tube where the pressure equals the vapor pressure, but immediately behind this area where the pressure is higher. Only if there exists a dual phase region (liquid and vapor) and at the same time a pressure difference $p - p_s = 0$ can primary reactions take place that lead to the destruction of materials (see Figure 2).

From the foregoing it is seen that the temperature factor by itself is not decisive in cavitation action; the emphasis must be placed upon the

pressure-vapor pressure relationship. In order to verify this further, cavitation tests were carried out with methanol, glycerin, and oils at subatmospheric pressures which entirely substantiate this conclusion. For methanol with $p = 380$ mm Hg and $p_s = 160$ mm, practically no damage could be noted after 10 minutes; for glycerin with $p = 380$ and $p_s = 0.002$ mm Hg considerable destruction took place but which, as expected, was less than that for $p = 760$ mm Hg. As a consequence of the very low vapor pressure of glycerin a feeble but discernible attack took place with $p = 8$ mm Hg. Viscous liquids such as oils show similar but much weaker damage when $p = 380$ mm Hg, p_s being at about 0.01 mm Hg. Later we shall deal with the influence of the gas content on this simple pressure relationship and the effect of surface tension and viscosity partly on the outer and partly on the inner conditions of the main reaction in the bubble compression. In order to test the validity of the relationship that exists between cavitation strength and vapor tension we tested a series of liquids within which the variation of surface tension (σ) and viscosity (η) was small (Table 2).

Table 2

Volume loss in aluminum with $\sigma \approx 22$ dynes/cm and $\eta \approx 6.6 \times 10^{-3}$ g/cm sec. after 52 minutes for equal amplitudes

Liquid	Density (ρ) g/cm	Surface tension (σ) dynes/cm	Viscosity (η) g/cm sec. (poises)	Temperature (° C)	Vapor pressure (mm Hg)	Volume loss (10^{-4} cm^3)
i-Amyl alcohol	0.81	26	0.009	0	0.6	4.5
Octane	0.70	22	0.006	15	9	4.8
Hexane	0.66	20	0.004	0	46	5.2
Methyl alcohol	0.79	23	0.007	20	96	6.3
Athyl alcohol	0.79	20	0.008	40	140	6.7
Cyclo hexane	0.78	24	0.007	40	180	7.4
Cyclo hexane	0.78	22	0.006	50	280	4.1
Cyclo hexane	0.78	20	0.006	60	440	2.4
Arbitrary	-	-	-	-	760	0

Figure 66 shows the weight loss as a function of the time. The values are somewhat scattered, partly due to conversion to the same vibration amplitude. But the characteristic path in Table 2 with the maximum value in the vicinity of $p_s = 180$ mm Hg for $p = 760$ mm Hg

remains intact. The values obtained for acetone (p_s = 150 and 230 mm Hg, respectively, σ = 23.5 and 22 dynes/cm, respectively) fit nicely into the above series, as do those for ethyl ether at low temperatures; here the weight loss is but little less (σ = 18 dynes/cm; the viscosity is about one-half). We believe that the influence of the viscosity is less than that of the surface tension.

Table 3

Volume loss in aluminum after 10 minutes of cavitation

Liquid	Density g/cm^3	Temperature (° C)	Vapor pressure (p_s) mm Hg	Viscosity (η) g/cm sec. poises	Surface tension (σ) dynes/cm	Volume loss 10^{-4} cm^3
N-Butonal	0.80	40	20	0.015	22	1.9
Water	1.00	20	22	0.01	70	7.4

14. The dependency of the cavitation attack on the surface tension and the viscosity of the liquid

A preliminary test was carried out with butanol at 40° C and water (Table 3). If one considers the influence of η and the density ρ as being inconsequential and the volume loss due to the influence of the surface tension alone, we have the graphic representation given in Figure 67 with $p_s \approx 10$ mm Hg. The values of the viscosities range between 0.007 and 0.04 g/cm sec. The results indicate that the surface tension is more responsible for the volume loss than the viscosity. This may be expressed:

$$\Delta V \sim \sigma - k\sigma^2,$$

That is, the strength of the primary reaction is linearly dependent on the surface tension since the released capillary energy is

$$A = 4\pi r_o^2 \sigma (r_o = \text{bubble radius before collapse}),$$

while the quadratic correction member refers to the outer condition which is still quite important in the primary reaction, even as viscosity and vapor pressure influence the vaporization and bubble formation, especially in regard to their numbers. If we convert the volume loss curve given in Figure 48 for water temperatures between 0° and 100° C, giving due regard to the influence of the surface tension, the maximum value leads to somewhat higher vapor pressures. With this we gain a still better view of the uniform course of the volume loss curve as a function of the vapor pressure.

At this point we might make comparisons of cavitation damage under different testing procedures. Volume loss as a function of time may be quite deceiving in evaluating the cavitation attack. As a matter of course initially strongly stressed test bodies become more strongly stressed with varying amplitudes, whereas weakly stressed test bodies have in the course of time a flatter volume loss curve even though the incubation period may be the same with the same kind of testing material. This must be considered in connection with the time volume loss curve, and testing time must extend well beyond this incubation period.

Cavitation tests carried out with water-alcohol mixtures are revealing. There is but little difference in the viscosities of the pure components and their solutions. Figure 68 gives the results, in which the surface tension as well as the partial pressures have been considered. With about 7 percent alcohol there is the greatest volume loss in aluminum test bodies. This loss is governed by the varying influence of p_s and σ. With an increasing proportion of alcohol there is an increase in the vapor pressure p_s and a decrease in the surface tension σ. The greatest changes occur in the region of small alcohol concentrations. From the steepness of ΔV with increasing p_s in Figure 48 we conclude that the influence of the vapor pressure exceeds that of the surface tension, shown in Figure 67. With an increase in alcohol concentration, however, the surface tension drops much more rapidly as the vapor pressure increases.

An evaluation as to the influence of the viscosity is more difficult, as viscous liquids usually have very small vapor pressures. The volume loss vapor pressure curve shows, however, the differences to be small in the volume loss for small vapor pressures, that is, for those below 1 mm Hg. Figure 69 gives the results of the weight loss in aluminum test pieces with respect to viscosity as well as saturation pressure for glycerin-water mixtures of various concentrations at a temperature of 28° C. There is not much difference in surface tension, 72 dynes/cm for water as against 63.5 dynes/cm for glycerin. Near 70-percent glycerin the maximum is flattened out. This is explained by the effect of the above mentioned vapor pressure, while a rise in loss with increased glycerin content speaks for a stronger attack with increased viscosity. The influence of the viscosity upon the cavitation strength is, however, certainly small:

$$F(\eta) = 1 \neq k' \eta,$$

where k' is very insignificant. In very viscous oils there appears a notable sheen effect. In this case the damage and surface tension are very small.

15. The influence of the gas content

Cavitation tests with varying gas content were first made by E. Spannhake (61) and later by Numachi (41). According to Böttcher (14) the gas content weakens, while according to Schröter (53) it strengthens cavitation action. The question comes up immediately in connection with the strength and type of damage at very-low vapor pressures, as there is

here the tendency to seek reactions other than those displayed with simple vaporization. In his observations of cavitation in the venturi tube the first author arrived at the view that merely the pressure head $p - p_s$ is diminished by the stress release through escaping air. Numachi proves the influence of air in water by changing the water pressure with the varying air content so that always a slight cavitation was maintained. The derived cavitation coefficient K_1 should, according to Numachi, be linearly dependent upon the ratio α/α_s, where α is the air content and α_s is the air saturation:

$$K_1 = \frac{p_1 - p_e}{q_e}$$

p_1 is the saturation pressure of the dissolved air, p_e the pressure at the start of cavitation and q_e the static head of the flowing water at the beginning of cavitation. For values $\alpha/\alpha_s > 0.8$ cavitation is brought about, there being no change when there is a transition to air-oversaturated water. In distilled water there is but a trace of air and even after a month α/α_s amounts to only 0.68. Schumb, Peters, and Milligan (54) found considerable difference in the damage caused in aluminum test pieces by ordinary and boiled methanol. However, our own comprehensive tests with water, methanol, ethanol, etc., have shown that there is no very marked difference in the damage caused by distilled liquids and those which were air saturated. Table 4 gives the weight losses in aluminum exposed to cavitation action for 10 minutes, the amplitude being constant.

Table 4

Weight loss in mg - aluminum in water at 25° C

Tap water	Distilled water	Tap water boiled for 1 hr.	Distilled water boiled for 1 hr.	Tap water with air*	Distilled water boiled for 1 hr. with air*
1.9	3.4	2.8	2.7	1.3	2.0

*Air was blown into liquid below test specimen.

If this behavior were formulated into a rule, then the gas content would most likely be considered as retarding cavitation. Stronger attacks on turbines during the summer when there is a diminished gas content substantiate this observation. The air content in water for various temperatures expressed as α (Bunsen's absorption coefficient) is:

Water	0°	20°	40°	60°	80°	100°
α	0.029	0.019	0.014	0.012	0.011	0.011

From this it also appears that the air content should have a weakening influence upon cavitation, although the erosion at first rises and then drops with gradually diminishing air. (Compare with characteristic weight (volume) loss-vapor pressure curve.) Since the nitrogen content of 0.002 g per liter water at 18° C drops to 0.001 g at 62° C, the number of bubbles and the cavitation damage rise disproportionally. It follows somewhat the exponential course of the vapor pressure in that region where the influence upon the tendency of the bubble film to spread across the surface of the test piece is as yet not so large. Table 4 shows that with lesser amounts of gas present greater damage results. It is difficult to decide whether the dissolved gas takes part directly in the primary reaction or is more of an outside condition influencing the number and type of singular erosions. However, we know that the primary reactions which are connected with the gas content are insignificant when compared with those of the vapor pockets.

Results obtained with mercury and glycerin are important. Here the quantities of dissolved gas are insignificant. Note the results observed when liquids and fusions are treated with ultrasonic waves, quickly expelling all the gas (49). Our experiments always showed the same bubble formation and accelerated vaporization regardless of the amount of air contained in the liquid. Ackeret (2) previously demonstrated that generally the quantity of the gases separated are insignificant as against the freed vapors. The strong hiss which always accompanies cavitation originates even at low temperatures (for example water at 0° C) from an accelerated vaporization. Careful measurements give observable differences in "vaporization" according to whether a liquid takes part in cavitation or not. One should, however, not assume that the accelerated vaporization is a consequence of ordinary mechanical squirting of the liquid. While treating ultrasonically liquid-gas systems such as benzol or water, Wood and Loomis (70) observed heavy fog formations even with oils of low volatility. They put a drop of oil on the end of a thin-walled glass tube connected to the ultrasonic transmitter and watched how the oil spread over the surface of the glass and was whirled away as fine fog. The oil does not run as a consequence of its weight but remains in a stable clinging condition. According to Bondy and Söllner (12) the causes for this behavior of the fog formation are supposed to lie in the cavitation. We observed a similar behavior, where in an experiment a drop of glycerin was held fast at the oscillating test body which was experiencing cavitation; the drop of liquid spread over the surface of the test piece and developed a symmetrical fog cloud. We find that in order to produce a characteristic attack it is not necessary to have an outer liquid surface for impact purposes; the procedure takes place in a liquid film which sets upon a vibrating base. Later we deal with what conclusion may be drawn from this as to the process going on in a venturi tube. Söllner showed (59) that the fog formation due to ultrasonic waves upon liquids can be explained only as the consequence of cavitation (hollow-space formation); furthermore he proved that the dissolved materials themselves go into fog with a disappearing vapor pressure. To be sure, it is noted that no fog formation takes place after a careful degassing (13). The bubble formation which proceeds rapidly at the boundary surface could, however, be introduced by the dissolved gases which

act as pores (vapor kernels) in the liquid. According to Bondy and Söllner, dispersion and with it cavitation does not occur in a vacuum nor at extremely high pressures.* As early as 1874, Kundt and Lehmann effected cavitation in completely degassed liquids by means of strong sound waves. This was accompanied by the clouding of the liquid and foam formation. In the formed hollow spaces which originate with the separation of the liquid,** the freed gas escapes as a consequence of the pressure decrease so that in a short time complete degassification is brought about. Bergmann (10) has shown that a viscous sugar solution in water containing much air can be completely degassed by means of ultrasonic waves, providing, as Sörenson has proved (60), they have the proper frequency. The smaller frequencies require higher energies. Therefore strong bubble formation can certainly be attributed to the accelerated vaporization or fog formation during which the vapor bubbles are formed, vibrate and burst. The hissing noise which always accompanies cavitation is explained primarily by the strong boiling action.

Boyle and Taylor (15) developed a formula*** for the sound-energy density with a point where all the energy is absorbed by the liquid and no cavitation takes place. This also is in accordance with our assumption that cavitation depends on pressure. The partial vacuum tests (Figure 65) show that only when $p - p_s = 0$ is there no cavitation. Even for very small outer pressures ($p = 8$ mm Hg) there is evidence of damage in liquids of low volatility such as glycerin and oils, while in liquids with lower boiling points such as water, benzol, etc., which are relatively gas free, no attack could be noted even after an extremely long time.

16. Formation of vapor bubbles and primary reaction

Rayleigh (45) was the first to calculate the pressures accompanying the collapse of vapor bubbles. He assumed that the formed hollow spaces were spherical. If p is again the outer pressure acting upon the bubble, r_o the original radius, r the radius of the compressed bubble and β the compression coefficient one obtains:****

$$\text{Pend} = \frac{2}{3} p \quad \beta\left(\frac{r_o^3}{r^3} - 1\right),$$

which gives pressures of many thousands of atmospheres. Using compression impact as a basis Ackeret (2) arrived at a pressure temperature relationship in vapor bubbles. At the beginning the inner pressure of the bubble

---

*At 2 atmospheres the dispersion is strongest. Gases in large quantities act as buffers.

**Tridimensional isotropic tension!

*** $e = \frac{(p - p_s)^2}{2\rho - a^2}$; p = outer pressure, p_s = vapor pressure, ρ = density, a = sound velocity.

****See Parsons and Cook (43), also (16).

is below the outer pressure, applied by the liquid flow; later on however, the inner pressure is far in excess of the outer, as a result of compression initiated by the original pressure difference $(p - p_i)$. Therefore, no equilibrium exists in the usual sense; the frictional forces are ignored. The possibility to calculate the inner pressure p_i depends essentially upon a knowledge of the heat condition of the bubble, the heat conductivity, and the time course of the hot vapors. For a nearly adiabatic compression of a bubble which with a stream velocity of 40 m/sec in a venturi tube, for example, collapses within a distance that is four times the diameter of the original bubble, a pressure some 2,500 times that of the outer pressure and a temperature of about 2,000° K is obtained. The preliminary condition for the bubble collapse lies in the very rapid outer pressure change. In contrast with the work of other investigators, Ackeret has under consideration water vapor bubbles and not gas or vacuum bubbles. Such large pressure changes are ever associated with rapid vibrations. This is in harmony with our observations in the oscillator experiment where the damage was always at the place of the vibrating vapor bubble, the degree of damage being a measure of the strength of the attack. According to the investigation of Smith (58) who studied the pulsation vibrations for small gas bubbles in the acoustic field, the local stresses are supposedly some 15,000 times that of the hydrostatic pressure. The resonance frequency is expressed by:

$$f = \frac{1}{2\pi}\sqrt{\frac{3x}{\rho}\left(p \neq \frac{2\sigma}{r}\right)} .$$

Here r is the bubble diameter, σ the density of the fluid, $x = \frac{c_p}{c_v}$, p the pressure, and σ the surface tension. With a frequency of 10 k Hz (10,000 cycles/sec) the critical r would be 0.3 mm! A. and E. Dognon and Biancani (17) also showed in their ultrasonic tests a considerable temperature rise in various fluids, leading the authors to ascribe an important role to the gas content. According to Bergmann (10), it is possible that adiabatic compression of air bubbles can cause a considerable local rise in temperatures. From the gas equation one obtains at a frequency of 1,000 k Hz (10^6 cycles/sec) with an amplitude of 4.4×10^{-4} cm a rise of some 239° C.

Later, van Iterson also explained cavitation and the damage which follows by the mechanism of collapsing air bubbles. As previously mentioned we have for equilibrium the relation:

$$p_i = p \neq \frac{2\sigma}{r}$$

where p_i is the inner pressure, p the outer pressure, σ the surface tension, and r the radius of the air bubble. Van Iterson assumes that the escape of the dissolved gas by the pressure drop is the cause of the cavitation phenomenon. He remarks that the symptom at the beginning of cavitation

is a certain noise which reminds one of gas being expelled from heating liquids. The energy which is set free in the collapse of an air bubble is determined by the capillary work:

$$A = 4\pi r_o^2 \sigma$$

(r_o = radius of bubble prior to collapse, σ = surface tension).
The forceful action is supposedly due to the bursting of the bubble which affects a very small surface since the contact angle of fast adhering bubble is but 4 to 6 degrees. In the explanation of the destruction process it is essential that the bubble stays fast at least momentarily during the compression. According to van Iterson the bubbles move quite slowly in a film layer and only the largest are thrown off and find their way into the liquid flow. This shows that there are exceedingly high excess pressures for very small bubbles inasmuch as the surface tension remains constant even as to bubbles of very small radii. Accordingly, one arrives at a critical radius since the dissolved air is set free when its pressure drops to that of the pressure of solution, according to Henry's law. The author makes his calculations with the assumption that the reabsorption of the air by the liquid takes place without resistance. He finds the time for disappearance of a bubble with a diameter of 10 mμ to be 10^{-6} seconds and for one with a diameter of 0.1 mm as 10^{-4} seconds. The path traversed by the small bubble with a water velocity of 12 m/sec amounts to 0.01 mm. The time rate of the compression and the subsequent impact pressure of the water become extraordinarily large with diminishing bubble radius. This is true even when more vapor bubbles than gas bubbles take part. This does not exclude the possibility of air containing vapor bubbles. From the hypothesis advanced by van Iterson concerning the rapid reabsorption of the air it would necessarily follow that by the collapse of the vapor bubbles there would be exceedingly rapid recondensation.

Ackeret and de Haller (5) succeeded in bringing about typical cavitation damage with the aid of a simple hydraulic impact apparatus without exceeding impact pressures of 6 atmospheres. They also assumed that the phenomenon involved neither gas nor vapor bubble formation, whether used with water or benzine. In spite of their specific statement that the pressure chamber always remained under a pressure of 7 atmospheres, we suspect that with the sufficiently rapid changes (16 impacts per second) there was on the return of the piston a reflected impact wave causing a stress release and bubble formation. In every case where cavitation appeared in the test, there was likely the primary reaction, a movement of a momentarily attached vapor or gas bubble, for which several proofs have been advanced.

Even Schröter pointed to the connection between bubbles and destruction and emphasized that a pure water stream in itself was insufficient. In the most impressive test, shown in Figure 37, the pronounced bubble formation is with moderate amplitude in the center of the test specimen, and a resonance bubble bursts with a change to a stronger vibration. If the vibration is suddenly stopped, the main damage is found to be exactly at the center. If the bubble, ordinarily in the center, is moved across the

surface of the test piece, the area of damage is more evenly distributed over the entire test body. Also in the venturi tube the destruction must be attributed to the fluid film studded with bubbles and vibrating on the material base and not to the rhythmically moving water masses or to the periodic constriction and widening of the liquid stream. A verification for this is found in the very long zone of damage behind the region of least pressure.

We now follow up the real primary reaction in the oscillating apparatus. Due to the inertia* of the surrounding water, the adhering vapor bubble is compressed and expanded to the rhythm of 10 k Hz (10,000 cycles/sec). This bubble can also collapse in a half period in the time of 10^{-4} sec. According to Ackeret this rapid change in the pressure is exactly the condition necessary for the bursting of vapor bubbles.

We now calculate the time required to collapse a bubble.** One with a diameter of 10^{-2} cm disappears in 10^{-5} sec. at a relative velocity of 4×10^{3} cm/sec, figured according to Ackeret's apparatus. With the oscillator, when the average amplitude is 0.05 mm and the average velocity of the piston some 5×10^{2} cm/sec we get a collapse time of 2×10^{-5} sec. which is still less than one-half the oscillating period. In the case of larger vapor bubbles, the pressure developed within the bubble and the temperature is even higher, allowing a total compression time of at least 5×10^{-5} sec. Due to the momentary adhesion of the vapor bubble during compression there is a transfer of heat to the test body, concentrated upon an exceedingly small area (0.1 μ x 0.1 μ and less) as a consequence of the high temperatures. In general, the compression process is polytropic, at any rate not quite adiabatic. In all probability the greater portion of heat is transferred to the surrounding liquid which as a consequence of the pressure drop at that place is again vaporized. This indicates that the heat of compression raises the temperature of this small surface area to a depth of a few atom layers. The fact that there are always localized rapid temperature changes points to the direct consequences of the primary reaction. This doubtless allows the possibility that the heat expansion of the material indirectly plays a part in the cavitation process. The localized temperature change is in turn dependent upon the specific heat and the heat conductivity. A possible outside influence is the property of chemical affinity--here the tendency of amalgamation (oberflächenverbindungen). This may have some bearing on the mechanism of compression depending upon

---

*It is impossible to consider water as elastic, solid material due to the exceedingly small relaxation periods of 10^{-16} sec., although there are accelerations at average amplitudes which are 500 times the acceleration due to the gravity of the earth. (See also Pohl (44)).

**By the vibrating bubble we do not necessarily mean one and the same bubble, since at the place where the bubble collapsed the instability of pressure and temperature create conditions favorable to the release of a new vapor bubble by further pressure.

whether the vapor bubble adheres lightly or more strongly upon the surface of the material. The impact of the liquid which follows the collapse of the bubble is upon a body which is not in its ordinary state and for this reason enormous static pressures are not required (see also G. Vogelpohl (69)). This also reveals why cavitation destruction could not be explained solely from observations of the mechanical properties of the material at room temperature.

In order to directly test the statements made, many experiments were carried out to measure these high temperatures with the very best thermocouples. As was to be expected, the results were negative since the inertia of the thermoelements was too great and its soldering too large in proportion to the area within which the action takes place. The circumstances are similar to those encountered by de Haller in his attempts to measure pressures with piezocrystals where only localized high pressures occur (25).

We include in the exterior factors all those influences which either increase or diminish the number and the extent of the primary reactions. In Figures 70 to 73 we show aluminum test bodies subjected to cavitation for 10 minutes with subatmospheric pressures and varying temperatures. The damaged area is fairly well defined; we may consider it that part of the test specimen with readily apparent destruction and excluding that part which to the eye appears free from damage. By plotting the diameters of these quite circular areas against the outside pressures, one obtains values for all tests which conform clearly to $p - p_s$. We find here also that, within wide limits, it is immaterial whether p for a certain value of $p - p_s$ is large or small. The maximum damage at $p = 760$ mm Hg is found when $p_s \approx 180$ mm and becomes smaller from there on. When $p = 550$ mm or less, the maximum destruction is always when the temperature is the lowest.

17. Chemical reactions in cavitation

In his cavitation tests at the Massachusetts Institute of Technology, in 1932, W. Spannhake observed the following:

> In a venturi tube with a 90 degree elbow one wall was reinforced with a 3 mm bronze sheet fastened with bolts. At the area where the bubble collapse took place there was always a pronounced tarnish. Furthermore, the bronze sheet stretched between the bolts and became warped. In the following year, Schröter (50 and 51) also noted this tarnish on brass bodies subjected to cavitation tests in venturi tubes.
>
> Such tarnish effects were later noted also in various steels and castings (Ebert and W. Spannhake (18)). It was found that steel subjected to a short test had a loosely adhering film of oxide or hydroxide which was of such thickness as to give a blue interference color. On longer exposure to cavitation action these oxide layers became very strong and anchored themselves into the metal. The tarnish colors become pronounced to the extent that they may be photographed with ordinary film. Figure 74 shows a non-annealed cast-malleable-iron test

specimen cavitated for 16 hours in a venturi tube; the oxide formation is visible at the light portion. One can note a varicolored ring system in the steel test body cavitated in the oscillator for 10 minutes in water, shown in Figure 75. Brittle metals such as cast iron, whose surface layer is not kneaded to any extent, retain this coloration even after long cavitation periods. This sheen is somewhat like that in very thin blades or like that of the colors in metals at high temperatures used as a rough temperature scale in metallurgy. This directly supports our hypothesis concerning the high localized temperatures (from the colors certainly higher than 250° C), since the layers of tarnish could not develop in so short a time under ordinary temperatures. In Figure 76 we may recognize where continued cavitation partly removed or cut through the oxide layer. With zinc we have dark-colored oxide layers. Especially pronounced is the oxidation of cadmium; the brown craters covering the area of attack are in the main cadmium oxide which could be determined immediately by X-ray analysis. The chemical attack as a secondary reaction in cavitation usually manifests itself by exposing the grain boundaries or by the strong action upon the variously arranged crystal surfaces. Figures 77 to 82 show some microphotographs of various metal test bodies (magnesium, antimony, brass, and steel) cavitated in water at room temperature. Such etchings could be obtained on specimens which had previously been polished. Upon the etched surfaces one may again observe localized damage due to primary cavitation action.

With respect to the chemical influence due to ultrasonics we refer the reader to the work of Bergmann (10).

IV. RESISTANCE TO CAVITATION

18. The change brought about at the surface of the material by cavitation

An understanding of the chemical influence, readily obtained from a study of the mechanism of the primary process leads directly to questioning the manner in which the destruction of the material takes place, whether it is purely mechanical, purely chemical, or a combination of both processes. By the primary process is meant the development of high localized temperatures in which the velocity of reaction K increases exponentially with $-\frac{B}{T}$, where B is a measure of the activating energy. Furthermore, one must determine whether in the mechanical destruction the individual impact or failure due to fatigue is responsible for the appearances that characterize cavitation.

One could present evidence that fatigue stresses are not to any extent involved in the purely mechanical destruction, for test specimens of pure magnesium subjected to cavitation for less than one-half second become damaged, as may be seen in Figure 83. After only one-half second plastic shrinkage may be observed and in some tests furrowed damages may also be noted. However, even in steel specimens, which have much greater cavitation resistance than magnesium, evidences of destruction may be observed in such short periods that would indicate that fatigue failure due to continuous stresses would be brought about after but a few thousand impacts. The shortest incubation period was perhaps one-tenth second, but here also a great number of points of attack could be observed. This indicates that at the beginning only the individual impacts are responsible since here the primary process is not accompanied by any strong secondary action. There is a variation in strength of these individual impacts in the different regions which is in harmony with the hypothesis concerning the primary process. This reminds us of the damage observed by Vater and Sorberger (68), which was caused by the individual impacts in the drop-impact apparatus.

With continued action there is the likelihood of the appearance of corrosion fatigue in addition to the mechanical fatigue stresses; for the strong pitting, which is the result of the primary process, provides many pronounced micropores that act as seats of chemical action. It is, however, impossible to explain the "initial" destructions on the basis of fatigue. The dual nature of the damage, that produced by the primary influence and that caused by fatigue, is exemplified in the cavitated zinc specimen (course-grained cleavage) in Figure 84. There one may see a darker part which consists of a brown oxide and a light-shiny part in which the free crystal surfaces are exposed, the result of fatigue failure in which large crystals have been split off (25 minutes corresponds to 15×10^6 impacts). The oxidized parts are due to the primary influence. From the development of the curve representing volume loss with time (Figures 8 and 28) one must assume that primary and secondary processes play a role in cavitation.

Disregarding ordinary corrosion conditions such as combinations of water and base metals which are not inactive, or mercury with metals soluble in it, the chemical attack may have two basic cavitation destruction methods: first, there may be a reaction of such magnitude as

to cause a loss in weight and for which the term cavitation corrosion is justified; second, there may be chemical attack without any marked loss of weight, acting to some extent as indicator of the primary process and having only an indirect influence upon the loss of volume (see also the additional discussion below). The first case may be considered as impossible for chemically resistant materials (glass, plastics, and gold platings cavitated in water); Fottinger and Bottcher each made reports on that.

Evidence that the chemical reaction is merely a side phenomenon in the microscopic destruction of materials is given in the series of Figures 85 to 87. The test body consists of a Mg-Ca alloy with 4.8-percent calcium prepared by polishing and etching with a dilute chromic acid solution. Figure 86 shows the test body being subjected to cavitation in glycerin after 1 seconds exposure. The weak but numerous points of attack that are distributed over the homogeneous magnesium crystal mixture (white in the picture) may be observed. At times these appear to be a multitude of chemical corrosion points. Morever, places at which shrinkage has occurred may be seen quite plainly,* especially strong deformations may be observed in the crystal marked Number 1 in Figure 87. A clue as how the weight loss is brought about may be had by comparing the three pictures showing the test body before cavitation, after being subjected to cavitation for 1 second, and for 2 seconds. At the points marked 2, 3, and 4 we note the severance of the mixed crystals from the eutectic alloy.** At point 2 there is a crystal which is partly severed (grain separation); in the immediate vicinity of this crystal very marked shrinkage may be observed in the mixed crystals. This comparison shows quite plainly the two stages in the destruction of a grain crystal. It is, however, not possible to make a definite statement concerning the attack upon the eutectic alloy.

At first we always encounter strong localized deformations and stresses (primary process) which subsequently result in the mechanical destruction (severance of a grain). It is the latter process which is responsible for the actual loss in weight. The continuous microscopic observation in the cavitation of steel gives some highly valuable information. The identical spots on the polished test bodies were investigated with the microscope at different intervals. Aside of the lines produced by the chemical etching, one sees here the micropores (also the crevices produced by polishing) which form the most favorable seats of the materials attack. The chemical effects noted as a side reaction in cavitation appears to come as a result of the enlarged surface area exposed, even in materials less resistive chemically. This area is in the form of protrusion points or edges which in turn act as favored seats at which vapor or gas bubbles are developed and to which they may adhere. Rjahskaja (46), too, recently arrived at the conclusion that the chemical

---

*The black spots seen in the picture are pores.

**The eutectic system consists of a crystal mixture rich in Mg and of Mg_2Ca.

reaction is not of importance in connection with the weight loss (see also (26 and 53)).

19. The behavior of metallic materials

A more thorough investigation of the damaged areas reveals that some have a shrunken appearance (are plastically deformed), while in other tests some areas give the impression of having been fused. The macrophotographs and microphotographs below are reproductions of cavitated magnesium and brass test bodies showing pronounced plastic deformations. In Figures 88 to 93 we see the line formations which are similar to those observed by Bottcher (14) and by v. Schwarz and coworkers (56). Of special interest is the macroscopic view of Figure 88 showing the varied manner in which shrinkage occurred in the differently orientated crystals. The crystallographically determined fissures and the direction in which they are most likely to develop are clearly seen in Figures 91 and 92. Strong transverse fissures are also visible in Figure 93. The attack takes place in such favored localities where twin streaks or grain boundaries occur and especially along enclosing borders or where the grains are less securely bonded. Figures 94 to 96 give an idea of the fusion effect in cavitation. In the macrophotographs of aluminum (Figure 27) and cadmium (Figure 94) there are the characteristic craters and the large fusion holes with surfaces, and especially ridges contrasting sharply with the less affected regions. In Figure 95 the peculiar tubercle-like formations are fusions which occurred in very small regions. This is a microphotograph of a magnesium specimen strongly cavitated in water. Cavitated Mg-Ca test specimens (4.8% Ca) also show fusions at places where mixed crystals are located.

For an evaluation of the primary cavitation attack (not, however, for a technical or practical strength evaluation) it is necessary that the attack be studied within very short periods, since soon after destruction takes place there is a strong overlapping of the primary and secondary effects. A definite physical characteristic of a material (for example the melting point) can be considered a contributing factor in the resistance to cavitation only for those processes which take place during the incubation period. The exponential increase in weight loss during the continued course in cavitation is explained by strengthened primary effects made possible by the previously damaged areas. An example of this is a magnesium test body, Figure 97, showing a multitude of small attack points within the larger previously formed craters.

In the vicinity of damages caused by individual impacts, whose magnitude depends upon the size of the collapsing vapor bubble, there appear at times unique chemical attacks, an example in a test body of monocrystalline antimony is seen in Figure 98. It may also occur after short cavitation period in steel specimens. The somewhat concentric oxide rings always appear in the same manner, irrespective of the method used. Figure 99 shows steel cavitated in the venturi nozzle. There is still doubt as to whether these local corrosions about the points of destruction are due to after reactions brought about by localized formations between the plastically deformed and nondeformed regions or whether they are the results of the high-temperature maximums. The latter assumption surely applies to brittle materials such as antimony,

and in all probability also to less brittle alloys as suggested by the many corrosion centers encountered after very short cavitation periods.

20. The behavior of nonmetallic materials

Of the nonmetals glass and plexiglass in water and ordinary salt in benzine were included in our cavitation experiments. The manner in which glass is attacked may be seen from Figure 100 which is 220 times enlarged. The effects of the individual impacts are in the form of small holes which only rarely are connected by fine-hair cracks. This demonstrates clearly that, generally, the primary process must take place within an exceedingly small region and that it must be very rapid since glass is considered a perfectly brittle material. Figure 101 shows a test body of plexiglass cavitated in water. Here the lines produced in the grinding process formed the seats of attack. The unique behavior of rock salt, cavitated in benzine, is well illustrated in Figures 102 and 103 where aside from the generally weaker attacks one may note typical fusions. Experiments with rubber, carried out by Schröter (51) in the venturi tube, showed that after but few hours the internal stresses were of such strength that the "rubber liquified inside and broke open at the outside."* The investigations concerning the behavior of rubber, leather, and similar materials in the high-frequency oscillator have not been concluded. The difficulty here lies in the proper fastening of the sample so that correct frequencies may be brought about. Many of these materials probably possess considerable sound absorption properties and it is possible that besides the actual cavitation destruction an inner structural disturbance may also play a part (10 and 28).

21. Structural change brought about by cavitation

After microscopic examinations disclosed that there was a separation of the crystalline grains when materials were subjected to cavitation stresses, attempts were made to investigate thoroughly the cleavage and structural relationships with the aid of X-ray interference. For this purpose we employed the reflected ray method, which had the additional advantage of high resolving powers. The particles remaining in the liquid are filtered and identified by the usual Debye method of analysis. The test bodies themselves are centered in such a manner so that they are near the axis of the camera with their front surface perpendicular to the main beam. The diameters of the X-ray camera were 57.3, 95.5, and 114.6 mm. In order to expose the identical region prior to and after cavitation, the test bodies were provided with bore holes at the sides with which to fasten them in the apparatus. (See Figure 22.) A refined copper target was used as the source of the rays and the area which was hit was about 1 mm^2. In these investigations we paid

---

*Vater and Sorberger (68) found that rubber behaved in the identical manner in the drop impact apparatus.

special attention to the homogeneity* of the test bodies, subjecting them to the shortest cavitation periods possible so that the layers in the region under observation were not too deeply affected. This insures that the penetration of the X-ray beam is in about the same relation as the depth to which the effects due to cavitation have proceeded. For the most diverse test bodies this was found to be almost exactly the same. As the consequence of cavitation the grain size of the main crystallites is diminished; this means they have been split, which agrees with the microscopic observations. The Debye lines of the cavitated materials are always compared in the same manner, contrasting them with the lines of the unaffected materials as shown in Figures 104 and 105 and Figures 106 and 107. The many individual points in Figures 104 and 106 representing reflection cones (reflex kegel) have largely disappeared in Figures 105 and 107, forming uniform lines. We can say that the size of the crystallites has changed from 10^{-3} cm to smaller crystallites whose magnitude is of the order of 10^{-4} to 10^{-5} cm. We found this splitting of the grains especially pronounced in a Mg-Ca alloy with 4.8 percent Ca which was cavitated in two stages (Figures 108 to 110). The single reflections in Figure 108 become progressively fewer in Figures 109 and 110. After the cavitation the strong reflections (large crystals) become considerably less in number.

Figures 111 and 112 show röntgenograms of a homogeneous Mg-Ca alloy with 0.45 percent Ca before and after cavitation. It may be noted here how the individual reflections of the fine-grained, originally highly oriented layers extend themselves along the Debye cones, which means that cavitation disorients the fine-grained materials. It is important that the separation of the $\alpha_{1,2}$-doublet remains intact even after cavitation, indicating an absence of any marked internal stresses. This demonstrates that relatively few regions of the entire cavitated zone disclose any strong deformations, which in turn is evidence that the action of the primary process is confined to minute areas while the macrodamage, exemplified by the separation of particles and the exposure of unstressed material, encompasses more or less the entire layer. The manner in which this disorientation is effected is well pictured in Figures 113 to 115, which show a copper test specimen at the beginning and after 30 and 120 seconds of cavitation. Similar results are obtained in experiments with monocrystals. At the beginning of cavitation the split crystal grains still maintain a strong directional orientation as expected. Figures 116 to 118, X-ray exposures of a salt crystal cavitated in benzine, show plainly the manner in which monocrystals behave on cavitation. The X-rays taken after cavitation are those of large pieces that had become separated. Therefore, the crystal orientation is not the same in each figure. The low strength of such a Na-Cl monocrystal permits the separation of fairly large pieces by a rather weak, uniformly distributed pressure. This separation process is furthered by the grooving of the test specimen with the sidewise turning in the removal of the sample.

---

*Homogeneity in the sense of equal grain size rather than theoretical phase homogeneity.

The investigation of the separated particles

With large amplitudes it is possible to pulverize the test material directly into the liquid so that a true suspension is obtained, for example, aluminum in water (see section 8). The residue of the aluminum, which was partly coarse grained, becomes very fine grained after cavitation in water, and using high reflection angles there is a splitting of the doublets, indicating that the particles eroded in the cavitation process have not undergone any marked deformation. In test samples composed of anisotropic crystals, such as zinc and cadmium, we find in the particles pronounced fracture surfaces which are distinctive for each material. By far the largest part of Al, Zn, and Cd which is worn off is pure metal. Only in the case of magnesium are there any appreciable amounts of oxides and hydroxides. This indicates that the processes causing the weight loss are much more of a mechanical than of a chemical nature. Chemical reactions, however, may serve as indicators for the stages through which the primary process runs.

The simplest way to prove the chemical attack is by the use of mercury as the cavitation medium. This affords at the same time an easy separation of the purely mechanical from the purely chemical influences (the mechanical influences as characterized by the primary effect and the mechanical secondary destruction). Steel samples cavitated in mercury show damage similar to but stronger than those cavitated in water. This strong destruction may be explained by the high surface tension ($\sigma \approx 500$ dynes/cm, see section 14) and the considerably higher density. Steel combines neither with liquid nor vaporized mercury and consequently does not go into a mixed crystal formation. Therefore, microscopic examinations show merely a large number of local attacks with plastic shrinkage (Figure 119). Here the region of attack is of greater extent than with water at low temperatures, which is quite understandable, since there is less adhesion of the vapor bubbles (with low affinity and no wetting property) and they can move across the surface much more easily. This action is furthered also by the larger active stream impulse.

However, if alloyable metals such as lead, cadmium, or copper are cavitated in mercury, there is besides the strong attack considerable amalgamation.* The velocity and the course of the alloying action is a suitable indicator of the conditions governing the primary process. A lead sample after 1 second of cavitation in mercury gives a mixed lead crystal. The two X-ray exposures, Figures 120 and 121, show clearly that we deal here with the homogeneous formation of a lead amalgam. The crystal lattice structure shrinks. This mixed crystal formation takes place with the utmost rapidity and only later on does weight loss set in. For comparison we might

---

*According to Schmid and Ehret (49), metals such as iron, chromium, etc., when subjected to ultrasonic waves become active in concentrated H_2SO_4 or HNO_3, while other metals such as aluminum, for example, become anodically more passive.

mention that the melting point of such a mercury-lead alloy lies between 260° and 290° C. To prepare this lead mixed crystal in such a short time thermically, temperatures far beyond this melting region would be required. In the cavitation of cadmium in mercury, the amalgamation occurs just as quickly before extensive destruction takes place. The cadmium mixed crystals formed in this process are like the solid metallic solution effected under a pressure of 50 atmospheres--percent cadmium (50 atmospheres multiplied by the percentage of the cadmium?) acting upon the upper surface of test piece for a few seconds. Also when copper is cavitated in mercury it appears as if some mercury is dissolved in the solid copper.

In the cavitation tests with mercury as the medium, the weight loss is affected in a large measure by the chemical attack. The unusually high reaction velocities with which these reactions take place and the rapid oxidations in metals and alloys also point to the extreme conditions which govern the primary process. Copper samples with thin films of gallium or with a covering of tin have been cavitated in water to determine the movement into the copper. In the latter case the tin layer was destroyed and separated too quickly to give any definite results. Gallium-covered copper samples showed that some gallium became dissolved by the copper. Especially pronounced was the dezincing of some brass samples which could be seen directly about the seat of the main destruction after but few minutes cavitation in water at room temperature. In samples of this sort it was easy to recognize zones of about 1/2 mm width which were red due to copper and not tarnish colors.

22. Cavitation resistance--its dependence upon the properties of the material--a look into the future

In section 8 we emphasized the characteristic course of the volume loss, which falls into two more or less definite regions:

(1) Cavitation during the incubation period where the only primary processes are active, producing microdeformations as well as chemical attacks. In one steel sample, subjected briefly to cavitation in the venturi tube, the oxide layers were thick enough to make a measurable increase in weight.

(2) Cavitation after the incubation period, with the appearance of a visible volume consumption brought about by the continued primary process and especially by its results--notch impact, permanent failure, and corrosion fatigue. At one time the primary process must be the cause of a destruction through temperature and pressure maxima at the place where a vapor pocket collapses. At another time it must cause localized stresses in the immediate vicinity of the collapse by the thermic expansion due to the unbalanced temperature distribution.* It is not at all surprising that X-rays

*It is possible that the stretching and swelling mentioned in section 17 is due to this cause. Surely, there is some connection between this and the apparent increase in strength during the incubation period which was observed by Schröter, Böttcher, v. Schwarz, and Mantel. It also throws some light on the reason why the property of cold forming is a measure of good cavitation resistance.

do not disclose any marked internal stresses since, in cavitation with the high-frequency oscillator, these regions are much too small compared to the separated particles. The volume loss taken after a sufficiently long time (relatively long with respect to the incubation period), is by itself an adequate practical criterion in the testing of materials. Since the weight loss is the result of a composite phenomenon, primary process and secondary attack, it is a much more comprehensive criterion concerning cavitation resistance than any single mechanical property, such as tensile or compressive strength. Materials with a low melting point, such as tin, lead, cadmium, and zinc, have but very little resistance as a consequence of the high localized temperature maxima; magnesium and aluminum occupy a somewhat more favorable position; brasses and steels display much greater cavitation resistance. The tensile and compressive strengths follow somewhat the same sequence. In Table 5 the volume loss after 10-minute cavitation with the same amplitude is given for pure annealed metals; also shown are their melting points and their tensile strengths (47).

Table 5

Volume loss for various metals due to cavitation

Cavitated material	Volume loss (mm^3)	Melting point (° C)	Tensile strength (kg/mm^2)	
			at 20° C	at 500° C
Lead (fine-grained)	10	327	1.35	-
Cadmium (fine-grained)	0.7	321	6.40	-
Magnesium (coarse-grained)	1.4	650	17.00	0.50
Aluminum (medium fine-grained)	0.5	658	14.30	0.60
Brass with 65% Cu (coarse-grained)	0.03	850	50.00	6.00
Carbon steel (fine-grained)	0.01 and less	1,150 to 1,500	54.00	27.00

The cavitation resistance for coarse-grained zinc lies between that of cadmium and magnesium. The table shows that there is some advantage to setting the cavitation resistance parallel to conditions existing at higher temperatures. Thus far the materials which have proved most resistant are the stellites, hard metals, austentitic and ledeburitic steels.

Additional factors of considerable influence are the size of grains and the number and size of the micropores. Highly porous steel and cast-iron specimens suffer strong volume losses. It is natural that the type of the crystal, whether homogeneous or heterogeneous, and the singular behavior of the various crystals* should have an appreciable

*According to v. Schwarz fine grains are considerably more resistant to cavitation than coarse textures.

influence. In this respect we are merely at the threshold of development. With the aid of the new testing procedures for abrasion a classification system might be arranged so as to take into account the structure and the composition of the better known materials and their effect upon the incubation period and any subsequent developments. Until then one can refer to the tables of Kerr (32) and of Mousson (36), which for practical purposes serve as guides in the design and construction of machine parts to be used where cavitation cannot be avoided.

Recently reports were published (57) of tests in which jets of water at extremely high velocities (1,000 m or 3,300 ft/sec) were able to cut through thick steel blocks in a very short time. To what extent this may prove useful in connection with cavitation studies remains to be seen.

As soon as cavitation takes place it is axiomatic that every material is attacked. Even the strongest and toughest are no exception and there is no possibility from the standpoint of materials to make provisions for complete protection against cavitation attack. To set up some standards for comparison with other types of stresses with respect to the degree of attack and the resistance of the material, we must consider that cavitation differs from mechanical stresses such as tensile, compressive or fatigue, which have a safety limit below which there is no failure. In cavitation, moreover, we have a typical wear process similar to corrosion or abrasion. Although sometimes of little practical significance because of its minuteness, this wear always occurs with any degree of cavitation, no matter how small. Therefore, the attempt to include cavitation into the category of fatigue stresses or corrosion fatigue cannot be entirely successful. The behavior of the material does not furnish any ready criterion as to what constitutes the limit of the fluid velocity below which no discernible cavitation damage takes place. These limits may be determined rather by the absence of the cavitation processes, especially the primary processes. Offhand it appears very unlikely that the cavitation increase should merely be proportional to the increase in the velocity of fluid (67). From the experiments with the high-frequency oscillator we have seen that the amplitude is a powerful factor. Thus, it is necessary to determine precisely the strength of the attack to arrive at some relative values generally true in materials testing for cavitation resistance. With respect to corrosion, this problem has already been solved; given the attacking medium, its concentration and temperature and the state of the liquid, whether at rest or in motion, the weight loss can be computed per unit area and per unit time. But how can one determine the strength of the cavitation attack? In what manner is the degree of attack observed in the oscillator to be correlated with that observed in the drop-impact apparatus, and with that in the venturi tube? And how is this to be carried over to practical machine construction? The extents of the areas involved in cavitation are hydrodynamically speaking very different, even in the same experimental procedure, as for example, in the oscillator. The volume loss in test samples of the identical material differing only in size cannot be discriminately compared. The measurements, therefore, give merely the relative values. An appropriate materials testing procedure, standardized for each type of testing, is an absolute requirement. In the drop-impact test a definite velocity and diameter of the jet must be determined, or the amplitude and acceleration

and the size of the test sample need to be standardized. In that manner a way might later be found to effect direct comparisons among the various water impact testing procedures, making possible the derivation of conversion factors from which the absolute strength of the cavitation attack in specified accelerations and frequencies may be defined.

V. SUMMARY

Besides giving a clear concept of cavitation, the first chapter describes the various testing arrangements, showing the cause of the materials damage by cavitation and the related water-hammer stresses. In the formation of vapor stress regions and the consequent materials destruction by flowing fluid there is always a dual phase region at the walls of the machine parts, namely liquid-vapor. The older concept of cavitation, which either demanded the presence of high pressures (impulse-like stresses caused by pressure waves) or else corrosion fatigue were not satisfactory. Mousson's and Ebert and Spannhake's cavitation resistance numbers for various materials showed no relationship to mechanical properties such as tensile and compressive strength, expansibility, or Brinell hardness.

Our cavitation experiments and those of others with Gaines' magneto striction oscillator are compared with the venturi-tube and the drop-impact tests (Tropfenschlaggerat). It appears that all three test methods gave essentially the same results. The time volume loss curves always show one slope within which the volume losses remain rather small. Also one always encounters in both the oscillator and venturi-tube method the line-like failure--direct proof of the existence of vibrating and collapsing vapor pockets (see Figures 57 and 62). In the same way the concomitant chemical reaction may be viewed as the secondary result of local energy concentrations in the collapse of the vapor pockets by the formation of oxide films (Figures 74 and 76); also the exposure of the grains in polished test specimens (Figures 12 and 79) by cavitation appears in both types of tests. In section 17 the venturi-tube and oscillatory tests show complete correspondence in the primary mechanism of the phenomenon of cavitation. Oscillator experiments determined the vapor pocket formation to be a direct reflection of the region of damage in the test sample. If the vapor pockets vibrate and break in the center, it is there that the seat of the major destruction is located, as is the case with water at room temperature (Figures 30 and 39). If on the other hand the pocket formation is confined to the border of the test specimen, the destruction occurs there (Figures 31 and 45). The strong influence of the vapor pocket relationship to the magnitude of the destruction is thus apparent. The influences of external and vapor pressure, surface tension and viscosity were also investigated. An increase in vapor pressure increases the number of vapor pockets and consequently the degree of destruction. On the other hand a diminished pressure difference eliminates the vibrating stable vapor pockets. This explains the experimental findings of Peters and his coworkers as well as our own results where no damage was suffered by test specimens in any fluid at or near the boiling point (sections 10, 11, and 12). The influence of surface tension is quite strong, i.e. liquids with great surface tension cause more damage.

In section 15 we found that absorbed gas has very little influence upon cavitation.

The high velocities of the chemical reaction and the large number of microscopic destructions indicate that the primary process is accompanied by local temperature peaks. Therefore, the impact on the minute area creates special attack conditions when the collapse of the bubble liberates capillary energy (section 16). This vapor pocket mechanism accounts for the porous surfaces being more susceptible to cavitation attack than smooth surfaces. The conclusions drawn from the low pressure tests are that the vapor pocket formations and not the fluid impact are responsible for cavitation action (Figure 65). With the external pressure reduced to the vapor pressure of water at room temperature no damage was suffered by a test specimen (sections 13 and 16). Under the action of cavitation the structural arrangement changes at the place of attack. Figures 85 and 87 show a shrinkage at the joints. Metals with a straight crystalline structure have their structure disorientated (Figures 113 and 115).

Fatigue and corrosion fatigue furthered by the strong indentations caused by the primary cavitation often cover the pits brought about by the cavitation. In some metallic tests this dual attack, primary cavitation, and permanent failure can be plainly interpreted (Figure 84). The volume loss is attributed to mechanical action and not chemical corrosion. Only with highly chemically active cavitation mediums, such as lead in mercury, is there greatly accelerated reaction (Figures 120 and 121).

There remains to be developed a general materials test for cavitation. The quality of cavitation resisting materials depends mainly on its crystalline structure. In the construction of hydraulic and marine machines attention should be paid to the use of such materials that will resist cavitation action or at least minimize it, since cavitation erosion cannot be entirely avoided.

- - -

LIST OF REFERENCES

1 Ackeret, J. Über Hohlraumbildung (Kavitation) in Wasserturbinen.
Escher-Wyss Mitt., vol. 1 (1928), pp. 40-45.

2 Ackeret, J. Experimentelle und theoretische Untersuchung über Hohlraumbildung (Kavitation) in Wasser.
Techn. Mech. Thermodyn. (Forsch. Ing.-Wes), vol. 1 (1930), pp. 1-22, 63-72.

3 Ackeret, J. Kavitation und Kavitationskorrosion. Lecture at Hamburg, 1932.
Hydromechanische Probleme des Schiffsantriebs, edited by G. Kemp and E. Foerster, pp. 227-240. Springer, Berlin, 1932.

4 Ackeret, J. and Haller, P. de. Untersuchung über Korrosion durch Wasserstoss.
Schweiz. Bauztg. vol. 98 (1931), p. 309.

5 Ackeret, J. and Haller, P. de. Über die Zerstörung von Werkstoffen durch Tropfenschlag und Kavitation.
Schweiz. Bauztg., vol. 108 (1936), pp. 105-6.

6 Ackeret, J. and Haller, P. de. Über Werkstoffzerstörung durch Stosswellen in Flussingkeiten.
Schweizer, Arch. angew. Wiss-Techn., vol. 4 (1938), pp. 293-94.

7 Allievi, L. Allgemeine Theorie über die veränderliche Bewegung des Wassers in Leitungen. Part 1, Rohrleitungen.
J. Springer, Berlin, 1909.

8 Barnaby, S. W. Formation of cavities in water by screw-propellers of high speeds.
Trans. Instn. Naval Archit., vol. 39 (1897), p. 139.

9 Belart, H. Die Kavitations-Versuchsanlage.
Escher-Wyss Mitt., vol. 4 (1931), pp. 65-70.

10 Bergmann, L. Der Ultraschall, 2d. Ed.
VDI, Berlin, 1939.

11 Beuthe, H. Über den Einfluss der Ultra-Schallwellen auf chemische Prozesse.
Z. Phys. Chem., Part A, vol. 163 (1933), pp. 161-71.

12 Bondy, C. and Söllner, K. On the mechanism of emulsification by ultra-sonic waves.
Trans. Faraday Soc., vol. 31 (1935), pp. 835-43.

13 Bondy, C. and Söllner, K. The influence of gases on mercury emulsions prepared by ultra-sonic waves.
Trans. Faraday Soc. vol. 31 (1935), pp. 843-44.

14 Böttcher, H. N. Die Zerstörung von Metallen durch Hohlsog (Kavitation).
Zeitschr. VDI, vol. 80 (1936), pp. 1489-1503.

Failure of metals due to cavitation under experimental conditions.
Trans. A.S.M.E. vol. 58 (1936), pp. 355-60.

15 Boyle, R. W. and Taylor, G. B. Cavitation in the track of ultra-sonic beam.
Phys. Rev. (II), vol. 27 (1926), p. 518.

16 Cook, S. S. Erosion by water hammer.
Proc. Royal Soc. London (A), vol. 119 (1928), pp. 481-88.

17 Dognon, A., Dognon, E. and Biancani, H. Ultra-sons et biologie.
Gauthier-Villars, Paris, 1937.

18 Ebert, L. and Spannhake, W. Bericht über Versuche von Materialprüfung bei Kavitationsangriff.
Karlsruhe T. H., 1938 (unpublished).

19 Englesson, E. Pitting in water-turbines.
Engineer, London, vol. 150 (1930), pp. 418-21.

20 Föttinger, H. Untersuchungen über Kavitation und Korrosion bei Turbinen, Turbopumpen und Propellern. Lecture at Göttingen, 1925.
Hydraulische Probleme, pp. 14-64. VDI, Berlin, 1926.

21 Föttinger, H. Versuche über einige typische Kavitationserscheinungen. Lecture at Hamburg, 1932.
Hydromechanische Probleme des Schiffsantriebs, edited by G. Kemp and E. Foerster, pp. 243-55.
J. Springer, Berlin, 1932.

22 Gaines, N. A magnetostriction oscillator producing intense audible sound and some effects obtained.
Physics, vol. 3 (1932), pp. 209-29.

23 Gardner, O. The erosion of steam turbine blades.
Engineer, London, vol. 153 (1932), pp. 146-47, 174-76, 202-5.

24 Haller, P. de. Untersuchungen über die durch Kavitation hervorgerufenen Korrosionen.
Schweiz. Bauztg. vol. 101 (1933), pp. 243-46, 260-64.

25 Haller, P. de. Untersuchungen über die Korrosionserscheinungen in Wasser-turbinen.
Escher-Wyss Mitt. vol. 6 (1933), pp. 77-84.

26 Haller, P. de. Erosion and Kavitations-Erosion.
Handbuch der Werkstoffkunde, vol. 2, pp. 471-88.
J. Springer, Berlin, 1939.

27 Honegger, E. Über Erosionsversuche.
BBC Mitt. vol. 14 (1927), pp. 74-95.

28 Hunsaker, J. C. Progress report on cavitation research at the Massachussetts Institute of Technology.
Paper presented at Int. Congr. Appl. Mech., Cambridge (England), 1934.

29 Hunsaker, J. C. Cavitation research.
Mech. Engng., vol. 57 (1935), pp. 211-16.

30 Hunsaker, J. C. Progress report on cavitation research at MIT.
Trans. A.S.M.E., vol. 57 (1935), pp. 423-24.

31 Iterson, K. F. H. van. Cavitation et tension superficielle.
Koninklijke Akad. van Wetenschappen te Amsterdam, vol. 39 (1936), pp. 138-48, 330-39.

32 Kerr, S. L. Determination of the relative resistance to cavitation erosion by the vibratory method.
Trans. A.S.M.E. vol. 59 (1937), pp. 373-97.

33 Kundt, A. and Lehmann, K. Über longitudinale Schwingungen in zylindrischen Flüssigkeitssäulen.
Pogg. Ann. vol. 153 (1879), pp. 1-12.

34 Mantel, W. Untersuchungen zur Erforschung der Zerstörung metallischer Baustoffe durch Wasserschlag.
Forsch.-Arb. über Metallkde. und Röntgenmetallographie, Folge 21, C. Hauser, Munchen, 1937.

35 Merrian, C. F. Progress in the study of cavitation.
Pennsylvania Water and Power Co., Baltimore, 1933 (unpublished).

36 Mousson, J. M. Pitting resistance of metals under cavitation.
Trans. A.S.M.E. vol. 59 (1937) pp. 399-408.

Untersuchungen über Hohlsog (Kavitation).
Zeitschr. VDI, vol. 82 (1938), pp. 397-400.

37 Müller, H. Kinematographische Aufnahme der Kavitation an einem Tragflügel. Lecture at Hamburg, 1932.
Hydromechanische Probleme des Schiffsantriebs, edited by G. Kemp and E. Foerster, pp. 311-314.
J. Springer, Berlin, 1932.

38 Müller, H. Kavitationserscheinungen bei Wasserturbinen.
Masch.-Schaden, vol. 12 (1935) pp. 188-92.

39 Müller, H. Spaltkavitation an schnell laufenden Turbomaschinen.
Zeitschr. VDI, vol. 79 (1935), pp. 1165-69.

40 Müller, H. Anfressungen durch Hohlsog und Tropfenschlag.
Stahl und Eisen, vol. 58 (1938), pp. 881-88.

41 Numachi, F. Über den Einfluss des Luftgehalts auf die Entstehung der Kavitation.
Ing.-Arch. vol. 7 (1936), p. 396.

42 Pagon, W. W. Paper for presentation at the annual meeting of the A.S.M.E., 1935 (unpublished).

43 Parsons, C. A. and Cook, S. S. Investigations into the cause of corrosion or erosion of propellers.
Engineering, vol. 107 (1919), pp. 515-19.

44 Pohl, E. Der Einfluss der Dampfnässe auf die Schaufeln im Niederdruckteil einer Turbine.
Masch.-Schaden, vol. 13 (1936) pp. 185-90; vol. 14 (1937), pp. 1-6, 37-43.

45 Rayleigh, J. W. S. (Lord). On the pressure developed in a liquid during the collapse of a spherical cavity.
Phil. Mag. (VI), vol. 34 (1917), pp. 94-98.

46 Rjashskaja, T. K. Kavitationswiderstand von Legierungen.
Metallurgist (Russ.), vol. 14 (1939), No. 12, pp. 50-56.

47 Sachs, G. Mechanische Technologie der Metalle.
Akad. Verl.-Ges., Leipzig, 1925, p. 201.

48 Schardin, H. and Struth, W. Neuere Ergebnisse der Funkenkinematographie.
Zeitschr. techn. Phys., vol. 18 (1937), pp. 474-77.

49 Schmid, G. and Ehret, L. Die Wirkung intensiven Schalls auf Metallschmelzen.
Zeitschr. f. Elektrochem. vol. 93 (1937) pp. 869-74.

50 Schröter, H. Korrosion durch Kavitation in einem Diffusor.
Zeitschr. VDI, vol. 76 (1932), pp. 511-12.

51 Schröter, H. Korrosion durch Kavitation.
Zeitschr. VDI, vol. 77 (1933), pp. 865-69.

52 Schröter, H. Werkstoffzerstörung durch Kavitation.
Zeitschr. VDI, vol. 78 (1934), pp. 349-51.

52 (Cont.) Versuche zur Frage der Werkstoffanfressung durch Kavitation. Forsch. Inst. Wasserbau u. Wasserkraft, K.-Wilh.-Ges. z. Förd. d. Wiss. Mitt. Heft 3. R. Oldenbourg, Munich and Berlin, 1935.

53 Schröter, H. Versuche über Werkstoffanfressung durch Kavitation. Zeitschr. VDI, vol. 80 (1936), pp. 479-80.

54 Schumb, W. C., Peters, H. and Milligan, K. H. A new method for studying cavitation erosion of metals. Metals & Alloys, vol. 8 (1937), pp. 126-32.

55 Schwarz, M. v. and Mantel, W. Zerstörung metallischer Werkstoffe durch Wasserschlag. Zeitschr. VDI, vol. 80 (1936), pp. 863-67.

Werkstoffzerstörung durch Tropfenschlag. Schweiz. Bauztg., vol. 109 (1937), pp. 225-27.

56 Schwarz, M. v. and Mantel, W. Die Zerstörung metallischer Baustoffe durch Wasserschlag. Korrosion und Metallsch., vol. 13 (1937), pp. 375-79.

57 Schwarz, M. v., Mantel, W. and Steiner, H. Tropfenschlaguntersuchungen zur Feststellung des Kavitationswiderstandes (Hohlsog). Z. Metallkde., vol. 33 (1941), pp. 236-44.

58 Smith, F. On the destructive mechanical effects of gas-bubbles liberated by the passage of intense sound through a liquid. Phil. Mag. (VII), vol. 19 (1935), pp. 1147-51.

59 Söllner, K. Experiments to demonstrate cavitation caused by ultra-sonic waves. Trans. Faraday Soc., vol. 32 (1936), pp. 1537-39.

60 Sörensen, ch. Absorptions-, Geschwindigkeits-und Entgasungsmessungen im Ultraschallgebiet. Ann. Phys. (V), vol. 26 (1936), pp. 121-37.

61 Spannhake, E. Kavitationsversuche am Massachusetts Institute of Technology und ihre Deutung. Zeitschr. angew. Math. Mech., vol. 14 (1931), pp. 374-78.

62 Spannhake, W. Erzeugung von Werkstoffbeschädigung durch Hohlsog bei schnellen Schwingungen fester Körper in Flüssigkeiten.
Zeitschr. VDI, vol. 82 (1938), p. 557.

63 Thoma, D. Die Kavitation bei Wasserturbinen. Paper read at Göttingen, 1925.
Hydraulische Probleme, pp. 65-74.
VDI, Berlin, 1926.

64 Thomson, W. On the formation of coreless vortices.
Proc. Royal Soc. London (A), vol. 42 (1887), p. 83.

65 Vater, M. Das Verhalten metallischer Werkstoffe bei Beanspruchung durch Flüssigkeitsschlag.
Zeitschr. VDI, vol. 81 (1937), pp. 1305-11.

66 Vater, M. Wasserschlag-Dauerversuche an reinem Eisen.
Zeitschr. VDI, vol. 82 (1938), pp. 672-74.

67 Vater, M. Verschleisswiderstand metallischer Werkstoffe gegen Sandstrahlbeanspruchung und gegen Hohlsog.
Zeitschr. VDI, vol. 82 (1938), p. 836.

Verschleiss and Wasserturbinen und Pumpen durch Hohlsog, Tropfenschlag und Sandschliff. Paper read at Stuttgart, 1938.
Reibung und Verschleiss, pp. 160-71. VDI, Berlin, 1939.

68 Vater, M. and Sorberger, W. Werkstoffzerstörung durch Wasserschlag bei Dauer- und Einzelschlag-Beanspruchung.
Zeitschr. VDI, vol. 83 (1939), pp. 725-28.

69 Vogelpohl, G. Untersuchungen über Korrosion bei Kavitation.
Zeitschr. VDI, vol. 77 (1933), p. 1099.

70 Wood, R. W. and Loomis, A. L. The physical and biological effects of high-frequency sound-waves of great intensity.
Phil. Mag. (VII), vol. 4 (1927), pp. 417-36.

Fig. 1. Shadow picture of cavitation action in Venturi tube, taken with simple spark (according to Föttinger [20]).

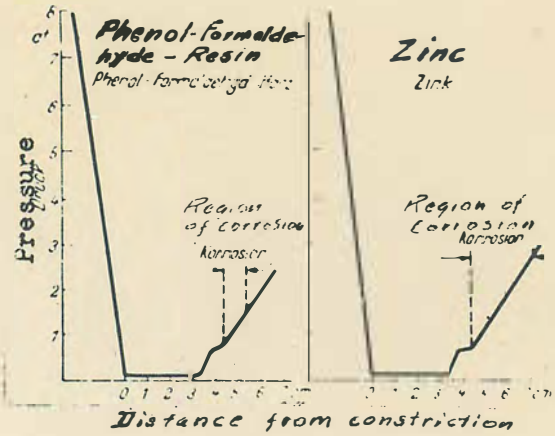

Fig. 2. Pressure distribution in Venturi tube - Region of destruction.

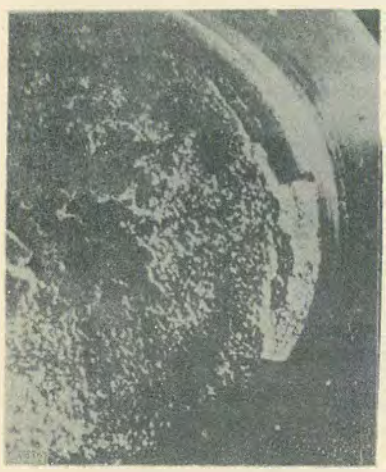

Fig. 3. Destruction in annealed cast-iron specimen subjected to cavitation in Venturi chamber (from Ebert and W. Spannhake, unpublished). One-half natural size.

Fig. 4. Test specimen subjected to cavitation attack in modified diffusor (according to Mousson [36]); natural size.

Fig. 5. Typical damage caused by water jet (according to Mousson [36]); four times enlarged.

Fig. 6. Destruction in bronze test body cavitated by oscillator (according to Kerr [32]); four times enlarged.

Fig. 7. Destruction in cast iron (according to Englesson [19]); 150 times enlarged.

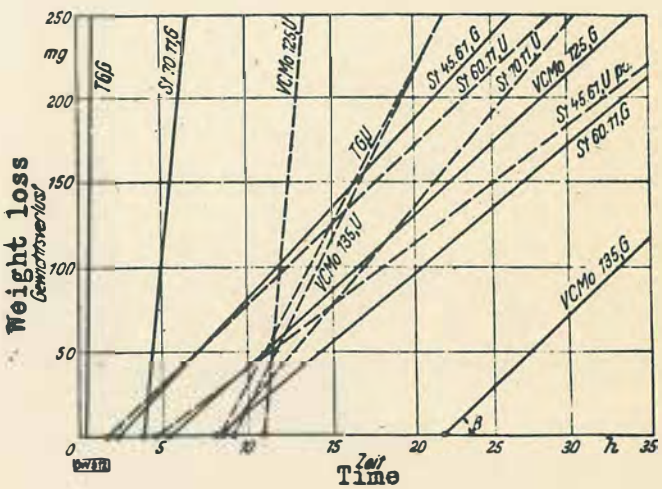

Fig. 8. Weight loss with respect to time in various test bodies cavitated in Venturi tube at Schwarzenbach plant. (From unpublished work of Ebert and W. Spannhake)

Water temperature 10° C.
Max. water velocity 80 m/sec
Length of diffusor 160 mm
Diameter of test bodies 40 mm
VCMo = high chrome-molybdenum steel
St = steel
PG = cast perlite
TG = annealed cast iron
affixed G = hardened
affixed U = nonhardened
tan B = rate of change

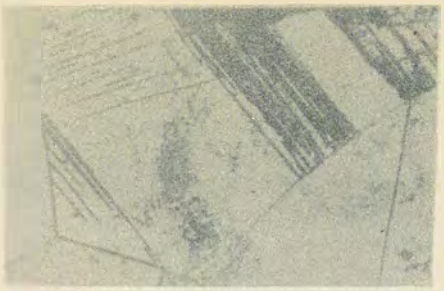

Fig. 9. Slip-lines formed in cavitated chrome-nickel steel; (according to Böttcher [14]); 140 times enlarged.

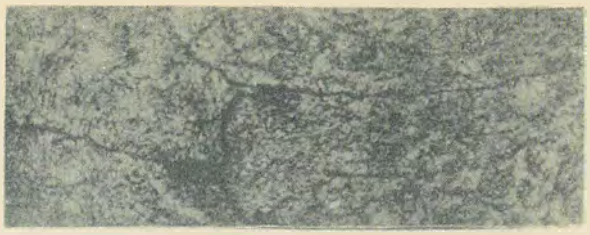

Fig. 10. Fatigue cracks in chrome steel as a result of cavitation (according to Bottcher [14]); 140 times enlarged.

Fig. 11. Grain exposure in a brass body cavitated in water (according to Schröter [52]; 10 times enlarged.

Fig. 12. Magnitude of destruction area in brass specimen (according to v. Schwarz and Mantel [55]); 260 times enlarged.

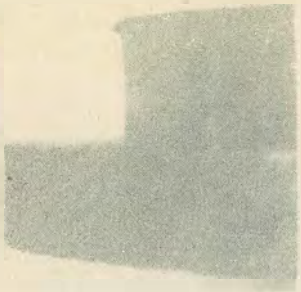

Fig. 13. Strongly deformed, annealed cast-iron specimen, cavitated in Venturi tube; at upper part of cylindrical specimen the plastic deformation is seen. (From unpublished work of Ebert and W. Spannhake) Natural size.

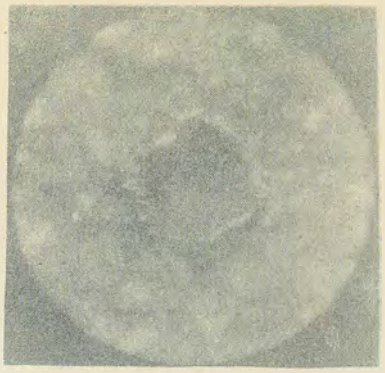

Fig. 14. Lead specimen cavitated in diffuser (Schröter [51]); 40 times enlarged.

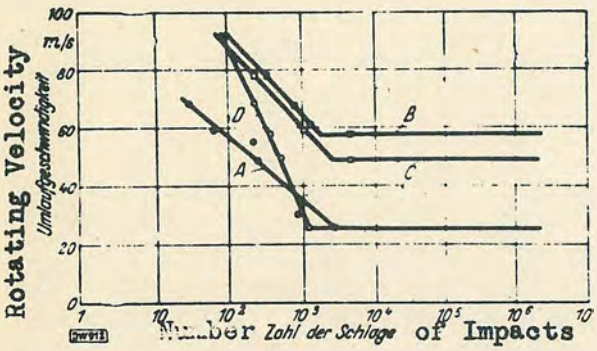

Fig. 15. Materials testing in drop-impact apparatus; representation of materials strength by Wöhler lines (according to Vater [65]).

A - pure iron; B - martensite steel
C - martensite cast steel
D - cast steel

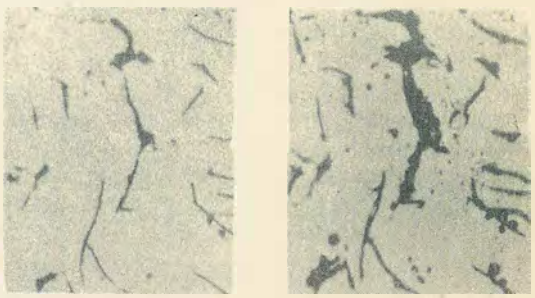

Fig. 16. Attack upon gray cast iron after 60,000 impacts with impact apparatus. 16a before test; 16b after test. (According to Ackeret and de Haller [5]); 120 times enlarged.

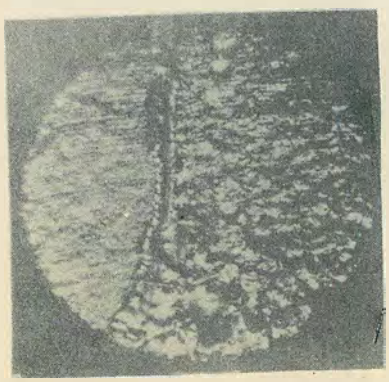

Fig. 17. Fused groove in lead specimen cavitated in Venturi tube. Note increasingly strong destruction to right of groove.

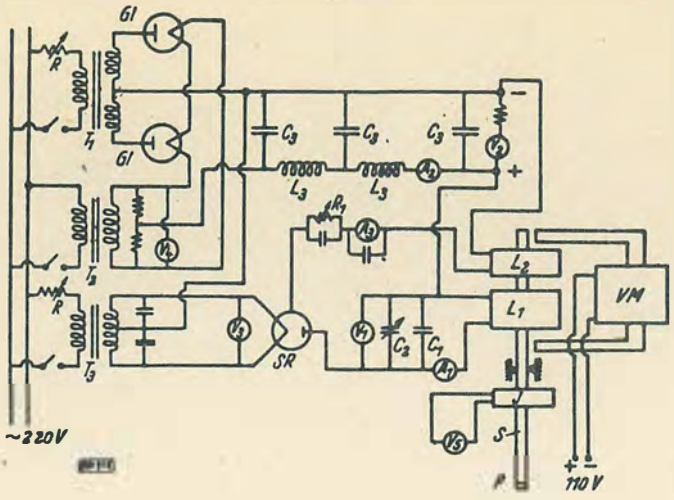

Fig. 18. Electric Diagram of Oscillator.

A_1	Ammeter for oscillating circuit
A_2	Ammeter for total current
A_3	Ammeter for grid current
C_1	Condenser for oscillating circuit
C_2	Variable condenser for oscillating circuit
C_3	Condensers for minimizing fluctuations in high-tension line
Gl	Rectifier tubes
J	Induction coil
L_1, L_2	Oscillator coils
L_3	Choke coils to minimize fluctuations in high-tension line
P	Test body
R	Variable resistances
R_1	Grid return resistance
S	Oscillating rod (tube)
SR	Transmitter tube
T_1	Transformer for high-tension conversion
T_2	Transformer for heating filaments in rectifiers
T_3	Transformer for heating filament in transmitter tube
V_1	Voltmeter in oscillating circuit
V_2	High-voltage meter
V_3	Voltmeter for heating of transmitter tube
V_4	Voltmeter for heating of rectifier tubes
V_5	Voltmeter for measurement of induction coil voltage

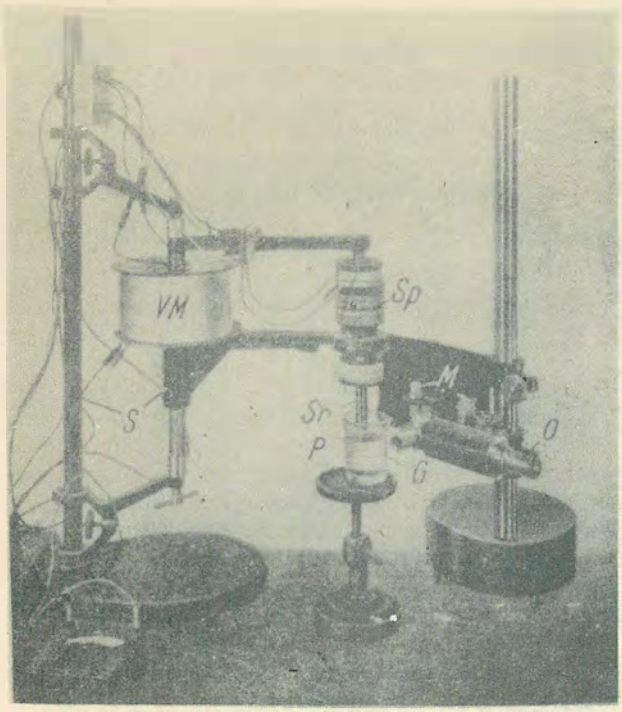

Fig. 19. View of oscillator with microscope.

G Beaker containing liquid
M Microscope
O Eyepiece
S Oscillator stand
Sp Oscillator coils
Sr Oscillator rod
VM Premagnetizing coil

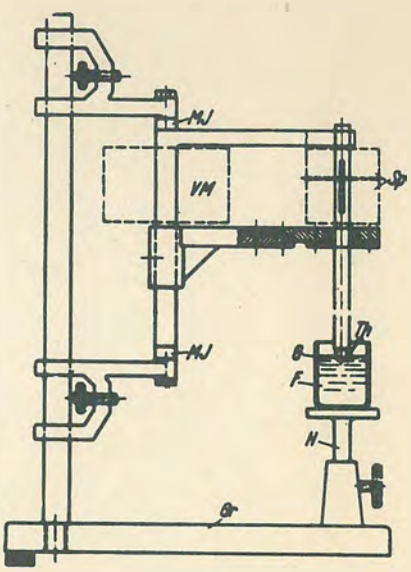

Fig. 20. Diagram of stand and fastening arrangement of rod.

F Cavitation liquid
G Container for F
Gr Base for stand
H Holding device
MJ Magnetic insulation
Sp Oscillator coil
Th Thermo element
VM Premagnetizing coil

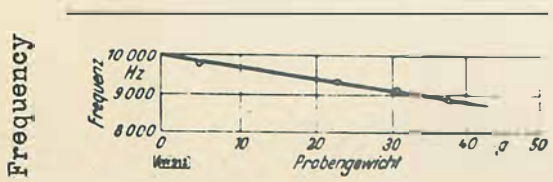

Weight of Specimen

Fig. 21. Frequency of oscillator as a function of weight of specimen.

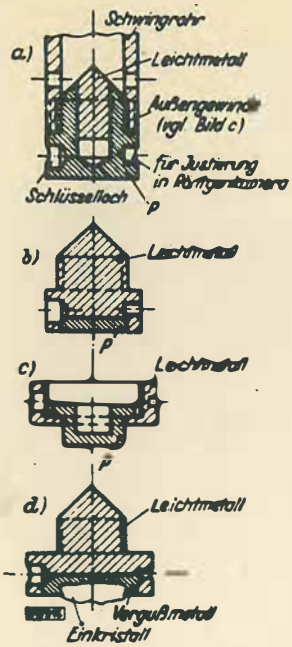

Key

Vibrating rod	
Light metal	
Outside thread	
For adjustment in X-ray camera	hole
Light metal	
Light metal	
Light metal	
Cast metal	

Mano crystal

Fig. 22. Shapes of specimens and methods of attaching them onto oscillating rod.

22a. Standard specimen.

22b. Specimen with inlaid heavy metal.

22c. Specimen for determination of weight loss.

22d. Specimen with inlaid crystal.

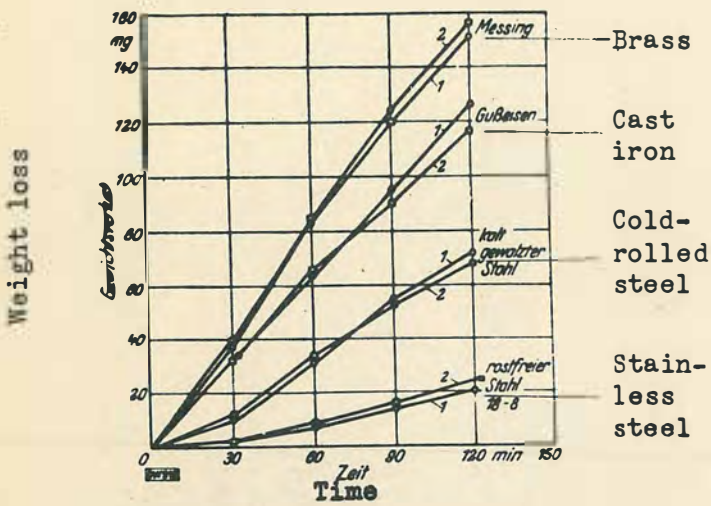

Fig. 23. Weight loss with respect to time of various materials cavitated in high-frequency oscillator at 20° C. Each type of material is represented by two different alloys. (According to Kerr [32]).

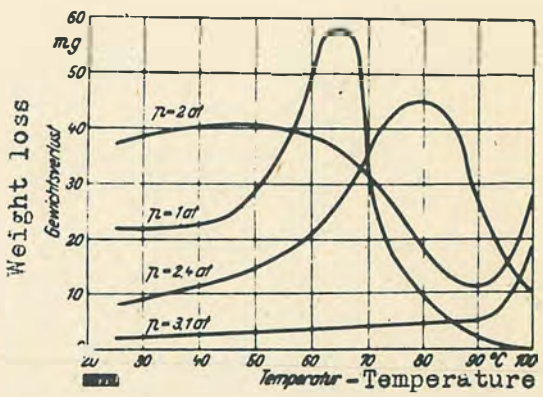

Fig. 24. Weight loss of brass specimens cavitated in high-frequency oscillator at various water temperatures. (From unpublished work of Peters and Rightmire)

Fig. 25. Nickel test specimen cavitated in oscillator (according to Gaines [22]); two times enlarged.

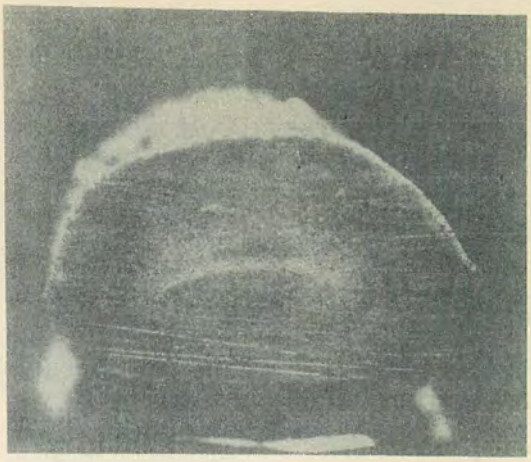

Fig. 26. Mg-Ca-alloy test specimen cavitated in oscillator; about natural size.

Fig. 27. Aluminum test specimen cavitated in water for 15 minutes; two times enlarged.

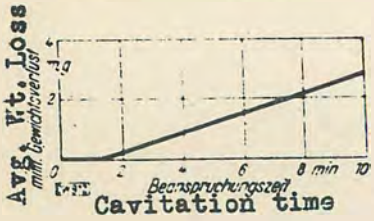

Fig. 28. Average weight loss with time, of magnesium test specimens cavitated in water from 0° to 100° C; amplitude, 0.06 mm.

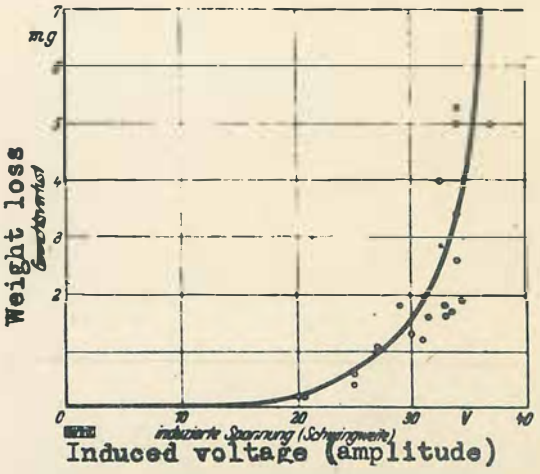

Fig. 29. Graph of weight loss with respect to amplitude of aluminum test specimens cavitated in water at room temperature for 10 minutes. (Induced voltage of 30 volts corresponds to an amplitude of 0.05 mm.)

Fig. 30

Fig. 31

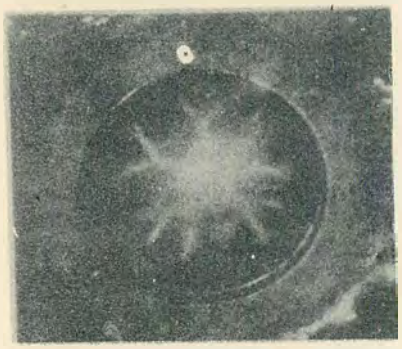

Fig. 32

Fig. 33

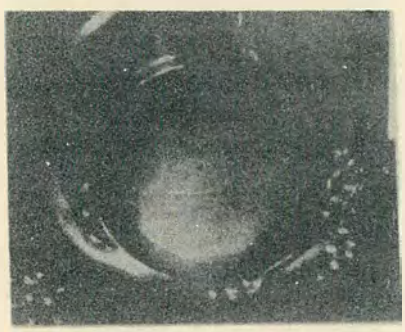

Fig. 34

Figs. 30 to 34. Bubble formation at surface of steel test specimens in various types of liquids.

Fig. 30. Distilled water at 20° C
Fig. 31. Distilled water at 80° C
Fig. 32. Benzol at 20° C
Fig. 34. Liquid paraffin at 20° C

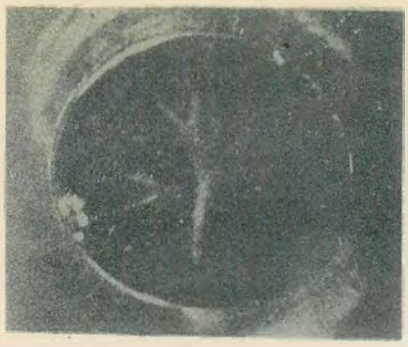

Fig. 35. Small amplitude.

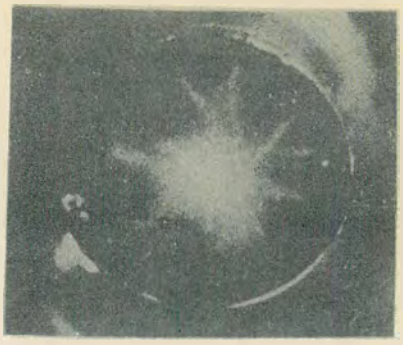

Fig. 36. Large amplitude.

Figs. 35 and 36. Bubble formation with two different sized amplitudes; about natural size.

Fig. 37a.

Fig. 37b.

Fig. 37. Bubble formation in glycerin at 1/4 second, (a); and at 1/2 second, (b). Sidewise view; about natural size.

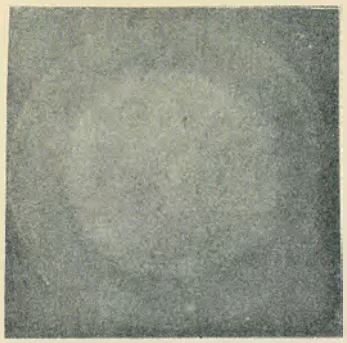

Fig. 38. 10° C

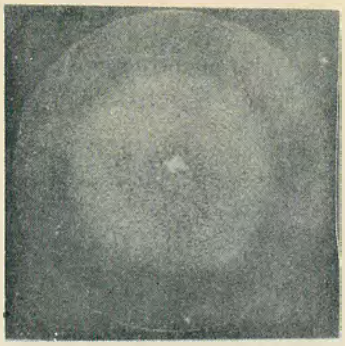

Fig. 39. 20° C

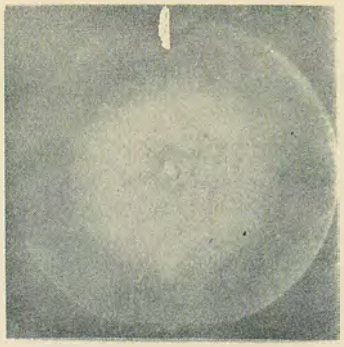

Fig. 40. 30° C

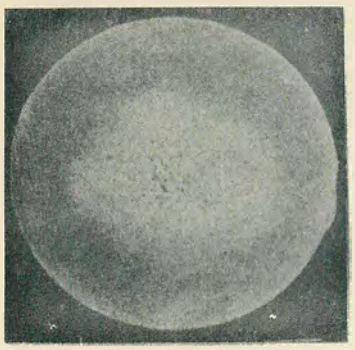

Fig. 41. 40° C

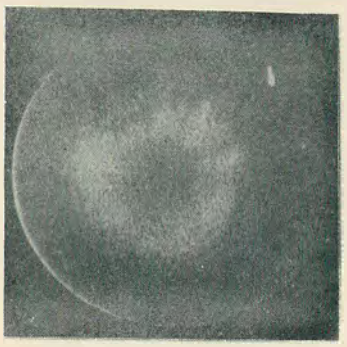

Fig. 42. 50° C

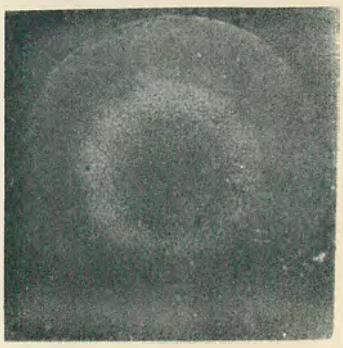

Fig. 43. 60° C

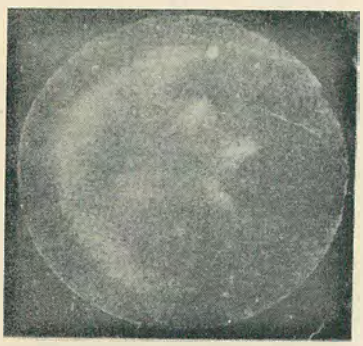

Fig. 44. 70° C

Fig. 45 80° C

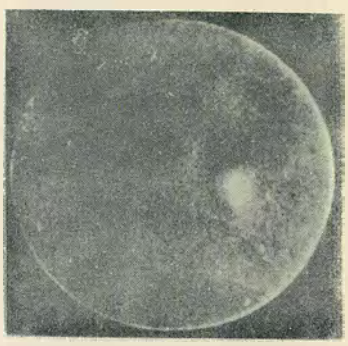

Fig. 46. 90° C

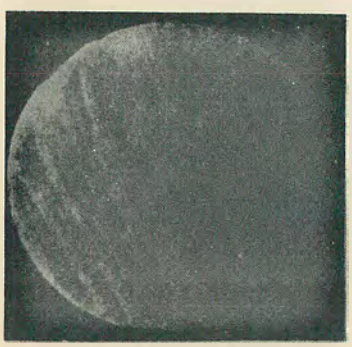

Fig. 47. 100° C

Figs. 38 to 47. Aluminum test specimens cavitated for one minute in distilled water at various temperatures, amplitude held constant; two times enlarged.

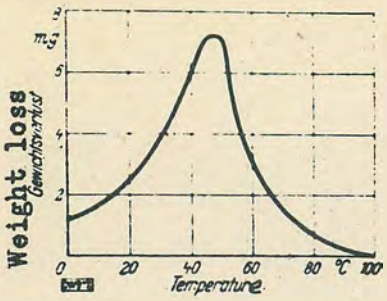

Fig. 48. Weight loss with respect to temperature; magnesium specimens cavitated in water for 10 minutes; amplitude 0.06 mm.

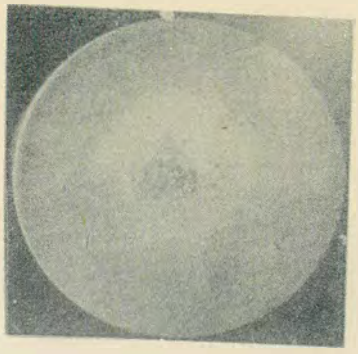

Fig. 49. Aluminum specimen cavitated in KOH (1/100 N) for 1 minute; two times enlarged.

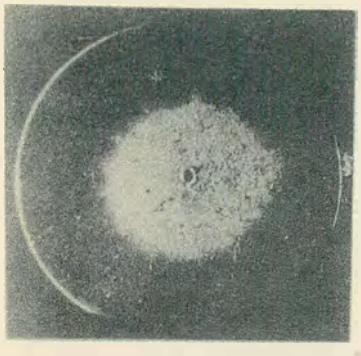

Fig. 50. Aluminum specimen cavitated in Na-Cl solution (1/100 N) for 1 minute; two times enlarged.

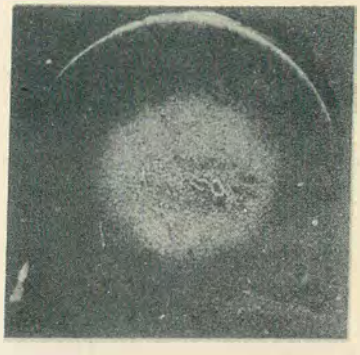

Fig. 51. Aluminum specimen cavitated in 30 percent hydrogen peroxide for 3 minutes; two times enlarged.

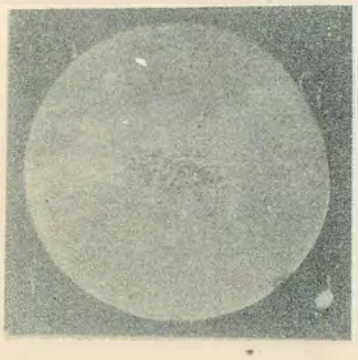

Fig. 52. Aluminum specimen cavitated in benzine (octane-nonane mixture) for 17 minutes; two times enlarged.

Fig. 53. Aluminum specimen cavitated in benzol for 17 minutes; two times enlarged.

Fig. 54. Aluminum specimen cavitated in ethyl ether for 17 minutes; two times enlarged.

	Boiling Point
Methyl alcoh	64.7° C
Ethyl alcoh	78.3° C
Cyclohexane	80.8° C
Heptane	98.4° C
Octane	125.8° C
Amyl alcoh	137.8° C

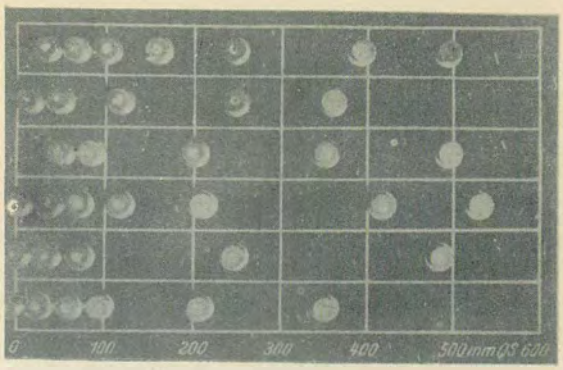

Fig. 55. Aluminum specimens cavitated in methyl alcohol, ethyl alcohol, cyclohexane, heptane, octane, and amyl alcohol at various temperatures (vapor pressures respectively); about 1/6 natural size.

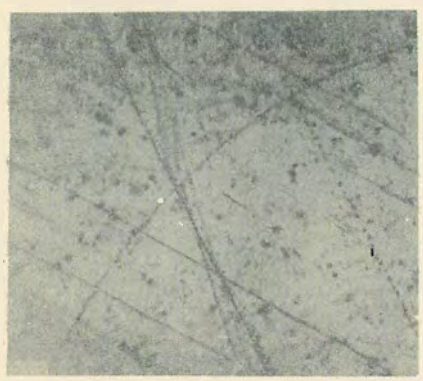

Fig. 56. 200 times enlarged.

Fig. 57. 400 times enlarged.

Figs. 56 and 57. Line-like microdamage in brass specimen cavitated in water for a short time.

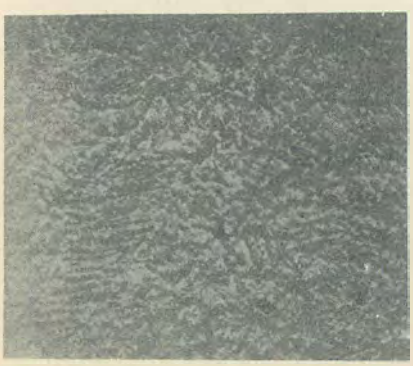

Fig. 58. Line-like microdamage in brass specimen exposed to cavitation action for a long time; 200 times enlarged.

Fig. 59. Line-like microdamage in antimony specimen exposed to cavitation action in water for a short period; 200 times enlarged.

Fig. 60. 100 times enlarged.

Fig. 61. 120 times enlarged.

Figs. 60 and 61. Line-like microdamage in heat-polished glass specimens cavitated in water.

Fig. 63. Damage in brass specimens cavitated in water under one atmosphere excess pressure at (a) 80° C, (b) 90° C, (c) 100° C; (from unpublished work of Peters and Rightmire); about natural size.

Fig. 62. Line-like microdamage in high alloy steel, cavitated in Venturi tube; 600 times enlarged.

Fig. 64. Arrangement for cavitation experiments under various outer pressures.

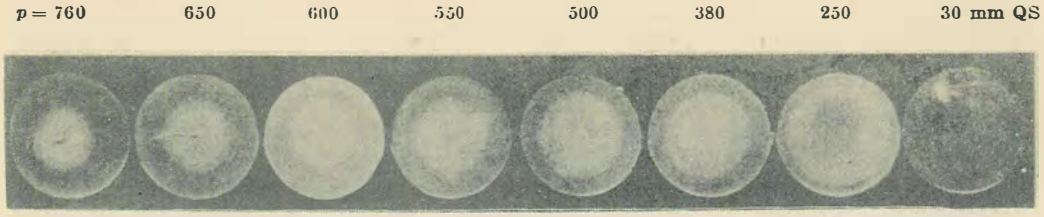

Fig. 65. Aluminum test specimens cavitated in water for 10 minutes under various outer pressures; about natural size.

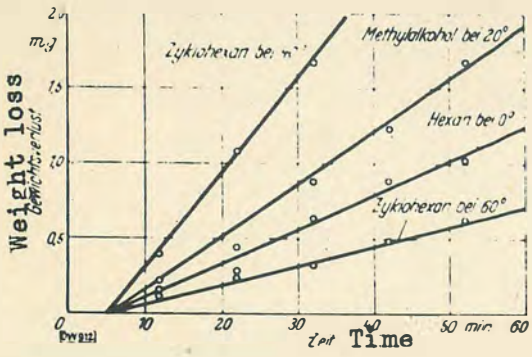

Fig. 66. Weight loss with respect to time in aluminum specimens cavitated in various liquids; amplitude 0.05 mm.

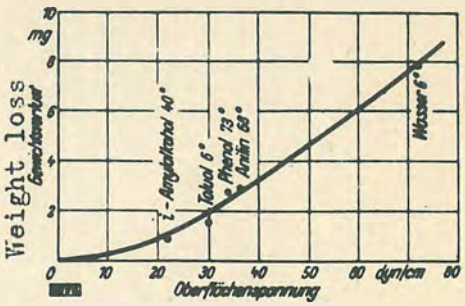

Surface tension

Fig. 67. Weight loss with respect to surface tension of aluminum specimens cavitated in various liquids; vapor pressure $p \approx 10$ mm Hg; viscosity η from 0.007 to 0.04 g/cm; amplitude 0.05 mm.

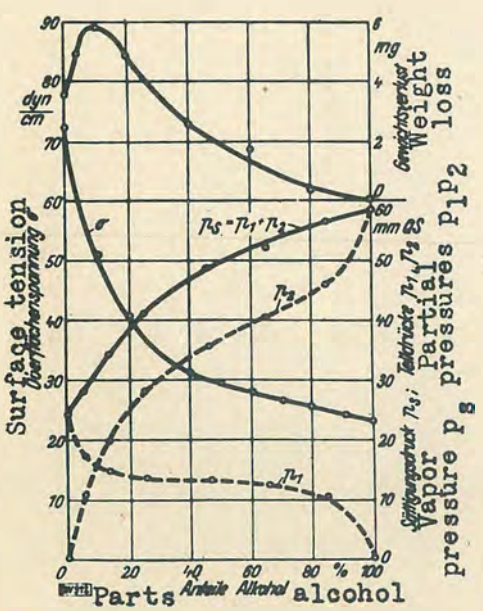

Fig. 68. Weight loss of aluminum specimens cavitated for 20 min. in water-alcohol mixtures at 25° C; also with respect to surface tension, vapor pressure, and partial pressures of water-alcohol mixtures; amplitude 0.05 mm.

p_1 partial pressure of water
p_2 partial pressure of alcohol

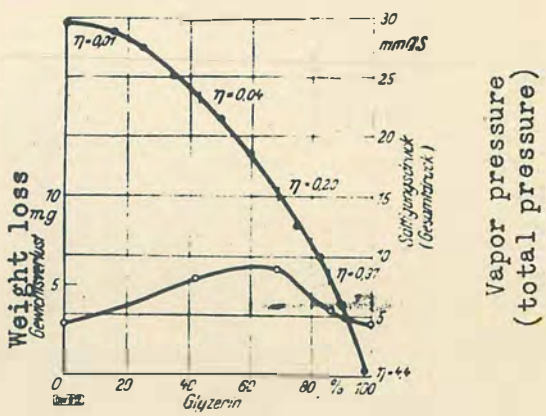

Fig. 69. Weight loss of aluminum specimen cavitated for 20 min. in water-glycerin mixtures of various concentrations; also with respect to vapor pressures and their associated viscosities; amplitude 0.04 mm.

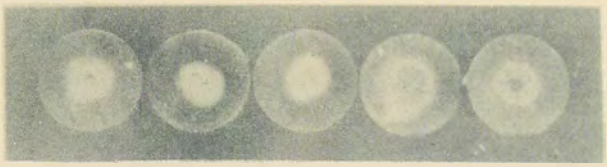

45° 61° 70° 79°

Fig. 70

40° 59° 72° 76°

Fig. 71

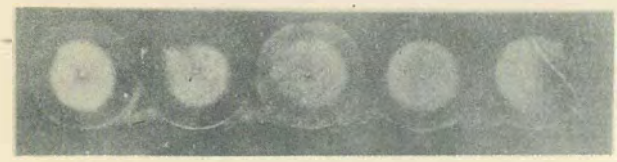

27° 45° 53° 67°

Fig. 72

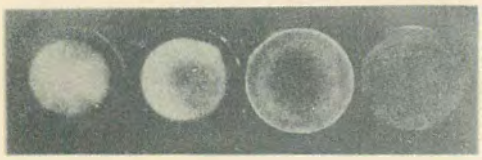

17° 26° 45° 51°

Fig. 73

Figs. 70 to 73. Cavitation of aluminum test specimen in water at various pressures and temperatures; about natural size.

Fig. 70. p = 760 mm Hg

Fig. 71. p = 650 mm Hg

Fig. 72. p = 450 mm Hg

Fig. 73. p = 360 mm Hg

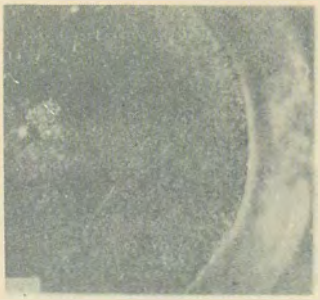

Fig. 74. Nonhardened cast-iron specimen cavitated in Venturi tube for 16 hours; (from unpublished work of Ebert and W. Spannhake); about 3/4 natural size.

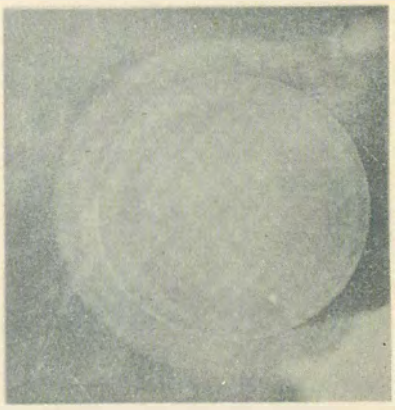

Fig. 75. Steel specimen cavitated 10 minutes in water with oscillator; about two times enlarged.

Fig. 76. Steel specimen after long cavitation; the partial removal of the oxide is plainly seen.

Fig. 77. Magnesium specimen cavitated for short period; 60 times enlarged.

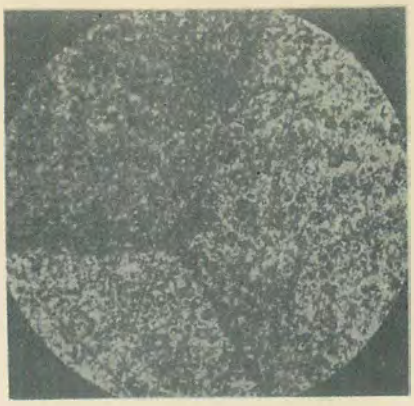

Fig. 78. Brass specimen, 53% Cu, cavitated for 10 min; about 100 times enlarged.

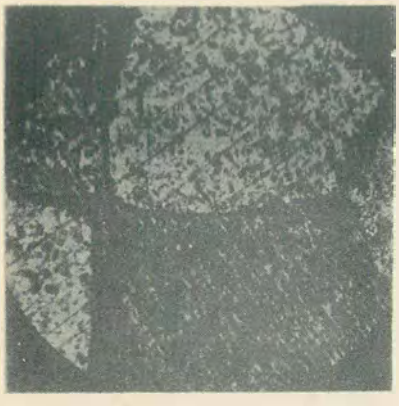

Fig. 79. Brass specimen, 58% Cu, cavitated for 10 min; about 100 times enlarged.

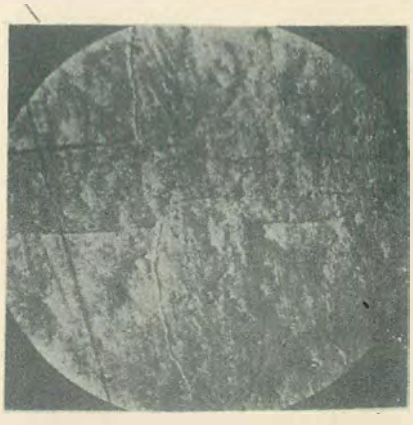

Fig. 80. Brass specimen, 65% Cu, cavitated for 8 min; (border zone); about 250 times enlarged.

Fig. 81. Antimony specimen slightly cavitated; 250 times enlarged.

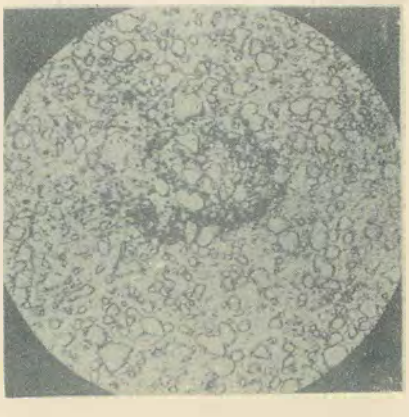

Fig. 82. High eutectoid steel specimen, strongly cavitated; about 400 times enlarged.

Fig. 83. Magnesium specimen cavitated in water for less than 1/2 second; 100 times enlarged.

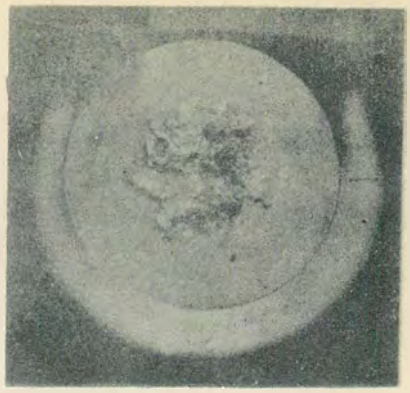

Fig. 84. Zinc specimen cavitated in water for 25 min; two times enlarged.

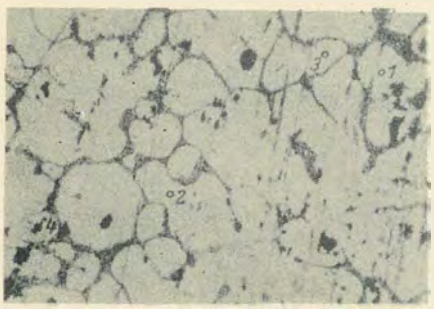

Fig. 85. Before cavitation.

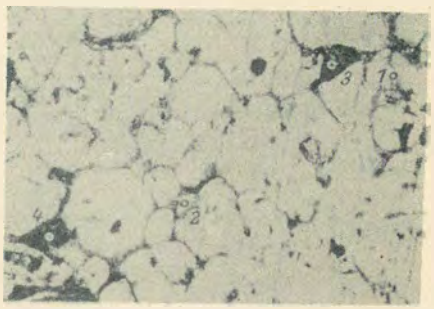

Fig. 86. After 1 second of cavitation.

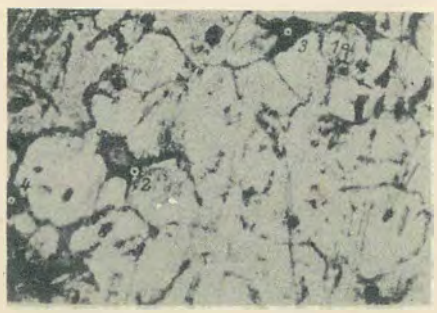

Fig. 87. After 2 seconds of cavitation.

Figs. 85 to 87. Microphotographs of Mg-Ca alloy cavitated in stages, in glycerin; 250 times enlarged. (The enumerated points indicate the same position.)

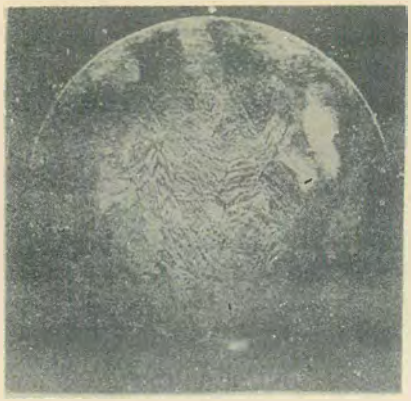

Fig. 88. Magnesium specimen cavitated in water for 10 min; two times enlarged.

Fig. 89. Brass specimen, 65% Cu, cavitated in water for 10 min; two times enlarged.

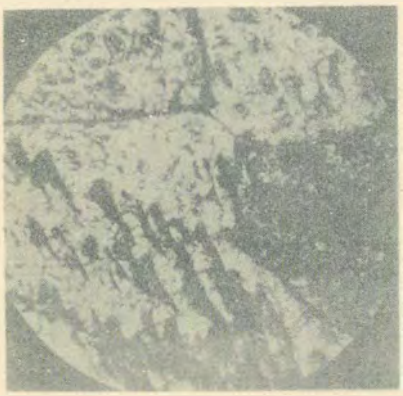

Fig. 90. Microphotograph of brass specimen shown in Fig. 89: about 70 times enlarged.

Fig. 91. Brass specimen cavitated in water for 4 min; 220 times enlarged.

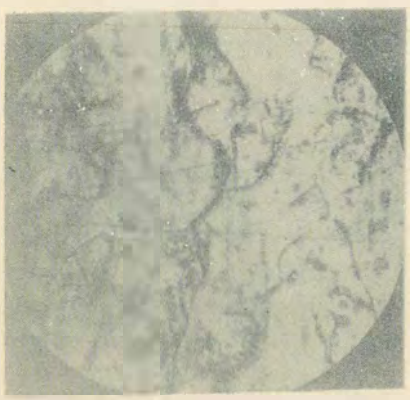

Fig. 92. Brass specimen cavitated in water for 4 min; 100 times enlarged.

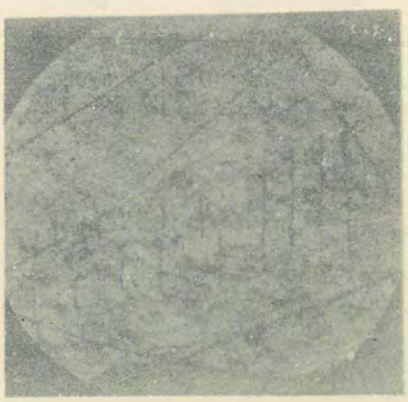

Fig. 93. Brass specimen, 55% Cu, cavitated in water for 12 min; (an added example showing the appearance of strong slippage lines); 220 times enlarged.

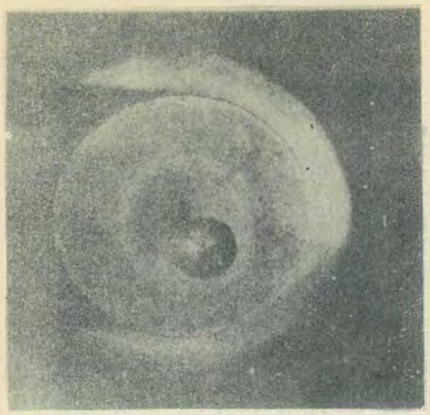

Fig. 94. Fusion cavity in cadmium specimen, cavitated in water for 1 min; caused by blowhole situated directly under the surface; about two times enlarged.

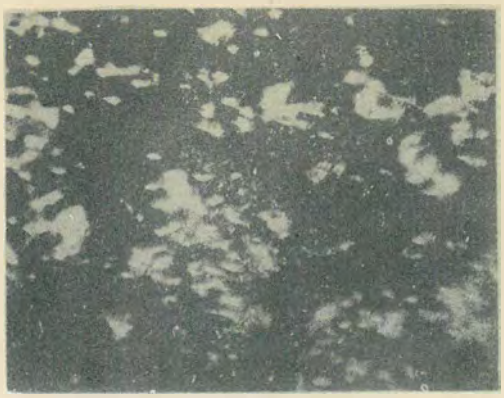

Fig. 95. Magnesium specimen strongly cavitated in water; 220 times enlarged.

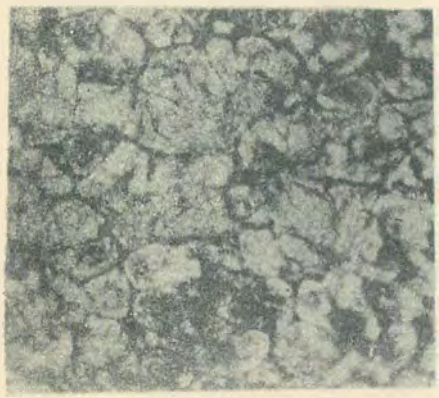

Fig. 96. Mg-Ca alloy with 4.8% Cu, cavitated in water for 15 min; about 250 times enlarged.

Fig. 97. Magnesium specimen cavitated in water 20 min; about 130 times enlarged. (Within the existing larger cavitation pits, smaller points of attack are visible.)

Fig. 98. Antimony monocrystal cavitated in water for 15 min; about 170 times enlarged.

Fig. 99. Steel specimen cavitated for 30 seconds in Venturi tube; (from unpublished work of Ebert and W. Spannhake); about 400 times enlarged.

Fig. 100. Glass specimen weakly cavitated in water; 220 times enlarged. (The strong damage in the center deserves special attention; the material behaved as though it had become plastic. The sharp edges ordinarily present in fractured glass are not present.)

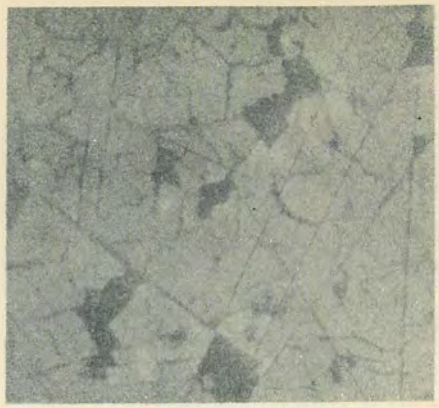

Fig. 101. Plexiglass cavitated in water for 1/2 minute; 220 times enlarged.

Fig. 102. Cavitated for 10 minutes; 220 times enlarged.

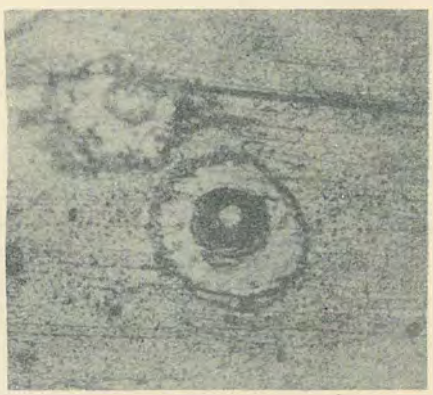

Fig. 103. Cavitated for 2 minutes; 100 times enlarged.

Figs. 102 and 103. Sodium chloride monocrystal cavitated in benzine.

Fig. 104. Before cavitation. Fig. 105. After cavitation.

Figs. 104 and 105. Reflected ray X-ray photos of Sn alloy specimen.

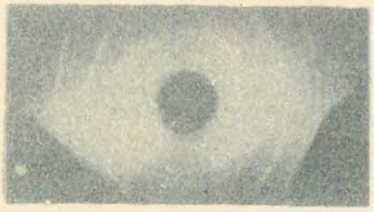

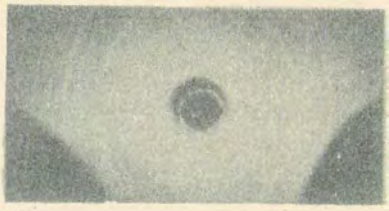

Fig. 106. Before cavitation. Fig. 107. After cavitation.

Figs. 106 and 107. Reflected ray X-ray photos of cadmium specimen.

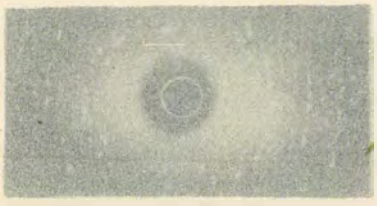

Fig. 108.

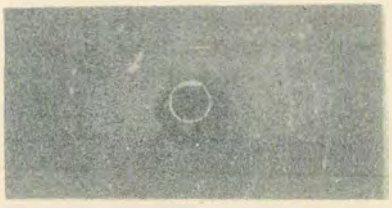

Fig. 109.

Fig. 110.

Figs. 108 to 110. Reflected ray X-ray photos of heterogeneous Mg-Ca alloy specimen.

Fig. 108. Before cavitation.

Fig. 109. Weakly cavitated.

Fig. 110. Strongly cavitated.

Fig. 111. Before cavitation.

Fig. 112. After cavitation

Figs. 111 and 112. Reflected ray X-ray photos of homogeneous Mg-Ca alloy specimen.

Fig. 113. Before cavitation.

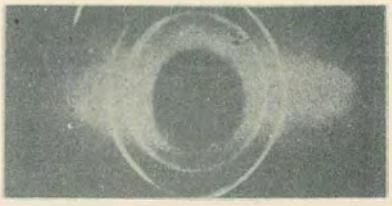

Fig. 114. Cavitated for 30 seconds.

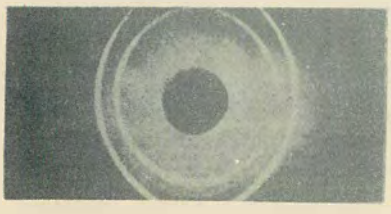

Fig. 115. Cavitated for 120 seconds.

Figs. 113 to 115. Reflected ray X-ray photos of copper specimen.

Fig. 116. Before cavitation.

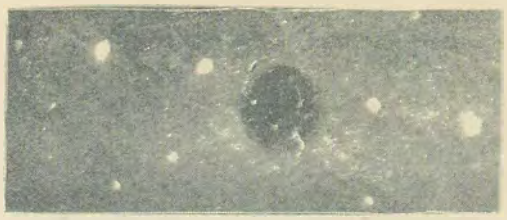

Fig. 117. Weakly cavitated.

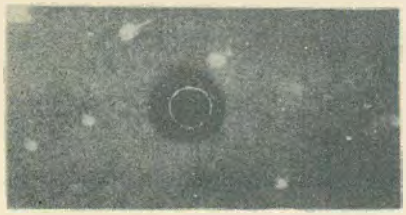

Fig. 118. Strongly cavitated.

Figs. 116 to 118. Reflected ray X-ray photos of rock-salt monocrystal specimen.

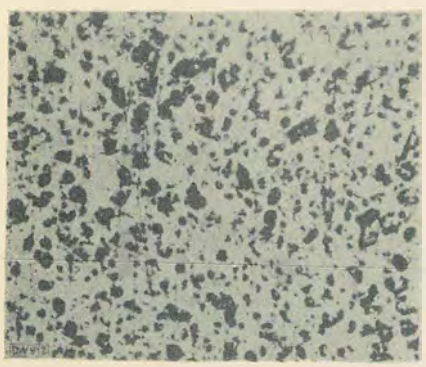

Fig. 119. Steel specimen weakly cavitated in mercury.

Fig. 120

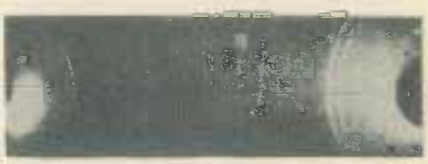

Fig. 121

Figs. 120 and 121. Debye-exposures of pure lead (Fig. 120) and of lead specimen cavitated in mercury for 1 second (Fig. 121).